Thermal Efficiency Enhancement for Future Rightsized Boosted GDI Engines - Effectiveness of the Operation Point Strategies Depending on the Engine Type

Thermal Efficiency Enhancement for Future Rightsized Boosted GDI Engines – Effectiveness of the Operation Point Strategies Depending on the Engine Type

S. Falfari, G.M. Bianchi, G. Cazzoli
University of Bologna
C. Forte
NAIS s.r.l.

ABSTRACT

Internal combustion engines are the primary transportation mover for today society and they will likely continue to be for decades to come. Hybridization is the most common solution to reduce the petrol-fuels consumption and to respect the new raw emission limits. The gasoline engines designed for running together with an electric motor need to have a very high thermal efficiency because they must work at high loads, where engine thermal efficiency is close to the maximum one. Therefore, the technical solutions bringing to thermal efficiency enhancement were adopted on HVs (Hybrid Vehicles) prior to conventional vehicles. In these days, these solutions are going to be adopted on conventional vehicles too.

The purpose of this work was to trace development guidelines useful for engine designers, based on the target power and focused on the maximization of the engine thermal efficiency, following the engine rightsizing concept. The originality of the present work stands in the comparison of the effectiveness of the most common strategies adopted today between two types of engine. The chosen engines for this study were modern boosted GDI engines, in line with the current automotive market, designed by CAD at the University of Bologna. 3D CFD computations of non-reacting flows were carried out by means Fire Code 2020 by AVL. The paper aimed to numerically investigate the rightsizing concept depending on the target level of power: two levels of power were chosen, 290 kW and 120 kW respectively, typical the former one of a high-power engine, the last one of an engine more devoted to efficiency purposes. The two engine bores were selected based on the common automotive solutions depending on the target power: 84 mm for the high-power engine, 75 mm for the other engine. Once fixed the bore value and pursuing the maximization of the thermal efficiency, a study on the possible geometries was performed, searching for the best stroke-to-bore ratio S/B: the long stroke engine design finds its limit in the maximum average piston speed, depending on the engine regime at maximum power. Then, the study was moved to the compression ratio increase and the adoption of over-expanded cycles, both aimed to increase the thermal efficiency. For solving the knocking issues arising from the adoption of increased compression ratio, the water injection strategy was analyzed too. Finally, some considerations were deduced on the effectiveness in applying the over-expanded cycles to the two different types of engine: the critical point to be solved is if the applicability and thus the effectiveness of the over-expanded cycles depend on the engine type.

INTRODUCTION

Today's car market must face increasing limitations on polluting emissions. This consideration is moving the automotive market trough 'more sustainable' technical solutions. Future engine design must consider different aspects: i) the continuous and progressive reduction of the allowed raw emissions; ii) the necessity in the next future of running the engine under stoichiometric conditions at full load conditions for limiting both the average and the local raw emissions, but at the same time keeping the Turbine Inlet Temperature TiT below the technological threshold value. In today's car manufacturers world, the key-factor is the thermal efficiency enhancement: it leads to a reduction in the consumption and leaves room to the rightsizing concept. In fact, the rightsizing concept, which is opposed to the downsized concept, leads to engines having:

1. More drivability, i.e. lower specific power and BMEP, maximum torque at low operation point. The BMEP reduction involves a reduction of the knock risk, which is the most limiting factor at full load conditions in modern engines;
2. More durability but at the expense of the fuel consumption. Anyway, the fuel might be saved adopting new solutions which pursue the increase of the thermal efficiency, as discussed below.

The necessity of reducing the raw emissions was addressed up to now following in the overall engine design the downsizing concept, which allows to reduce the Brake-Specific Fuel Consumption (BSFC) through the reduction of the total engine swept volume. At the same time, the automotive market imposed car manufacturers to keep constant the target power, moving toward engine solutions characterized by high specific power and high load, which involve high knock risk. Moreover, the new test cycles WLTP and RDE were found to be characterized by many points at full load / full power: for limiting the TiT value below the technological limit imposed by current turbine technology, up to now the solution was to run the engine under rich conditions, exploiting the evaporation of fuel to cool the mixture. At this point, it is necessary to tackle this tricky point in the short and long term perspective. It is very likely that in the short term future this strategy will not be allowed anymore because it is responsible of local peaks

of raw emissions, especially CO, but it will be replaced by the stoichiometric condition, which ensures the maximum conversion rate for the Three-Way Catalyst TWC: today the average of each individual polluting specie is computed over the entire test cycle, while in future it will be measured and limited locally for each point of the test cycle. It means that each polluting specie will have to stay always below a certain limit, even locally during the test cycle: peaks of polluting species will not be allowed anymore. The loss in the mixture cooling effect due to the smaller amount of injected fuel, which is a consequence of the shift toward strategies characterized by stoichiometric mixtures instead of rich ones, induces a high knock risk at full load conditions: this critical issue might be fixed by adopting 'operation point' strategies, which might be very demanding, some especially for the turbo-chargers, such as over-expanded cycles, cooled EGR, water injection, Turbulent Jet Ignition (TJI).

In a long term perspective of ICE application, the increase of the overall engine efficiency is mandatory. As a contribution to that the first step is enhancement of the engine thermodynamic efficiency η_{TH}. In the case of SI engines, the well-known ideal Otto-cycle definition of η_{TH} is used:

$$\eta_{TH} = 1 - \frac{1}{CR^{k-1}} \quad (1)$$

Where *CR* is the compression/expansion ratio, *k* is the specific heat ratio of the fluid. For a given target power, the engine theoretical thermal efficiency improvement can be pursued as follows:

a. Geometric compression ratio (CR) increase (or variable CR solution). This solution leads to a theoretical thermal efficiency gain and then to a TiT reduction but involves concerns about knock risks at high load/high engine speed conditions.
b. Expansion ratio increase, obtainable by adopting over-expanded cycles (Miller, Atkinson), which also have the advantage of reducing the average temperature of the mixture at TDC, reducing the knock risk at high load/high engine speed.
c. Mixture index λ increase:

$$\lambda = \frac{1}{\Phi} = \frac{A/F}{A/F_{STECH}} \quad (2)$$

The increase of the mixture index enhances the specific heat ratio *k* and thus the theoretical thermal efficiency.

Turning now to the actual thermal efficiency of the engine, the indicated and adiabatic efficiency must be considered because of the effect of real engine operation which includes [1]: i) current (retarded) combustion timing because of knock at large load ii) pumping loss; ii) heat rejection; iii) exhaust enthalpy loss; iv) unburned mixture. By pursuing the increase of the effective thermal efficiency of the engine which will always be referred to in the following as thermal efficiency, the geometric solution of increasing the stroke-to-bore ratio (S/B) is a valuable option: the engine efficiency is increased by the stroke enhancement, which leads to a more suitable surface-to-volume ratio (Su/V), capable of reducing the wall losses. Moreover, the combustion rate is enhanced because of both the increased turbulence (linked to the longer stroke) and the most favorable surface-to-volume ratio of the flame front exhibits a larger effective surface. The lower heat rejection trough the chamber walls results in a drawback because it determines the increase of the mixture temperature which, in combination with an increased CR, could lead to knock issues at high load. Lastly, the above cited adoption of lean mixture leads to the increase of the thermal efficiency thanks to the reduction of the heat losses through the cylinder walls and/or piston surface. In order to sustain the flame speed under lean conditions the adoption of high-tumble ducts for enhancing the turbulence generation process is pursued. It must be outlined that the lean operation option is currently mainly limited by the increase of costs since a De-NOx aftertreatment must be installed in exhaust line.

The adoption of solutions aimed to increase the thermal efficiency of the engine makes it possible to adopt the engine concept of the rightsizing, which represents an alternative to the downsizing concept: the idea is to find the best geometrical sizing of the engine depending on the target maximum power, as it will be shown next in the paper. Rightsizing is a response to downsizing, which is common in the automotive industry: downsizing means construction of smaller engines, i.e. with increased specific power and Brake Mean Effective Pressure BMEP for keeping constant the target power. In the last decade, lower fuel consumption began to become an increasingly important parameter of the engines in the European market, being the macro-parameter in addressing the emission limitation [2]. Rightsizing was born for commercial vehicles because the modern downsizing trend for cars cannot be directly transferred to commercial vehicles: in this concept, the engine is adapted to the size of the vehicle, at the expense of a slightly higher fuel consumption, which can be reduced looking for other ways to reduce fuel consumption, apart from reducing the engine capacity, such as the just cited improvement of the engine efficiency.

LITERATURE SURVEY

About the actual thermal efficiency enhancement, in [3] the authors highlighted as currently Atkinson cycle, cooled EGR (Exhaust Gas Recirculation) and low friction technologies are commonly adopted resulting in a thermal efficiency close to 40%. In the next future much higher thermal efficiency will be required, close to 45%, which needs more efforts: long stroke engine design with high tumble ducts, lean boosted concepts together with cooled EGR were investigated in [3]. Actual engine thermal efficiency results from various losses, such as mechanical loss (reduced by low friction strategies), pumping loss, cooling heat loss (reduced by long stroke design), exhaust loss (reduced by adopting over-expanded cycles) and unburned loss, which need to be decreased. The last generation engine adopts cooled EGR (it contributes to enhance the engine thermal efficiency extremely because it mitigates engine knocking and reduces cooling heat loss due to lower temperature combustion), electric water pump and low friction technologies. For thermal efficiency enhancement the authors in [3] adopted various strategies:

i) Stroke-to-bore ratio increase: it is limited to 1.5 because of limitation to engine speed and valve size. The stroke-to-bore increase allows to decrease the Su/V ratio, getting low heat losses and enhancing combustion process.
ii) High tumble port adoption. The long stroke engine also enhances the air flow and the air turbulence in the combustion chamber to promote combustion.
iii) High discharge current ignition aimed to expand the combustion limit in the strong air flow field, avoiding the quenching of the ignition flame.

In [4] authors collected gross indicated, net indicated, and brake fuel conversion efficiencies at various compression ratios from several sources. They highlighted that if engines are downsized in order to maintain constant the maximum torque and at the same time the compression ratio is increased, the relative increase in brake efficiency is about 1.6 times. In [5] authors studied the potential of jet ignition as an enabling technology for ultra-lean SI combustion to significantly increase thermal efficiency and to reduce BSFC and NOx emissions. Parametric studies were done in [6] using engine experiments and GT-Power engine simulations. The effects of boosting and downsizing, retarding spark timings, and increasing compression ratios on the fuel economy of a passenger vehicle and a light-duty truck were analyzed. In [7] authors highlighted as the combination of geometrically variable compression (VCR) and early intake valve closure (EIVC) proved to offer high potential for increasing efficiency of gasoline engines. For the application of over-expanded cycles, a decisive role is played by the valve train: the variability of valve trains has increased in the last few years, allowing to both shift the valve lift curve and to vary the valve lift curve in terms of lift height and opening/closing points. In [8] both the EIVC and LIVC cams were found to benefit the engine efficiency by reducing pumping work at part load and suppressing knocking at high load. Recent technologies offer significant improvements to the efficiency of turbocharged GDI engines [9, 10, 11]: Miller Cycle via late intake valve closing (LIVC), low pressure cooled EGR, port water injection (PWI), and cylinder deactivation. The authors have compared these technologies to each other on the same engine at a range of operating conditions and over a range of CRs, both numerically [10] and experimentally [11]. In [12, 13] the authors for better understand how the Atkinson cycle and the Miller cycle influence the fuel consumption at different engine speeds and loads, compared the influence of early intake valve closing (EIVC) and late intake valve closing (LIVC) on the fuel consumption of a 1.5L turbo-charged gasoline direct injection (TGDI) engine. Wan et al. [14] for improving part load performances proposed the study of over-expanded (Atkinson/Miller) cycle, which uses late/early intake valve closing (LIVC/EIVC) to reduce pumping losses in part load operation, combined with high geometry CR.

Many authors studied water injection application on modern S.I. GDI engines, starting from the main properties of the water [15, 16]. The anti-knock attitude of the water, related to its high cooling effect, was experimentally and numerically assessed [17, 18, 19, 20, 21, 22], also highlighting the consequent flame slowdown [23].

PAPER FOCUS AND FRAMEWORK

The originality of the present work stands in the comparison of the effectiveness of the most common strategies adopted today between two types of engine, focused one on high efficiency and the other on performance. In particular, the aim of the work was to trace development guidelines useful for future engine design as a function of:

1. Target power: two target powers were identified, one suitable for engines designed for high-power density, the other for ‘more efficient’ engines. The BMEP value was kept almost the same for the two engines.
2. Engine type, identified by the engine parameter stroke-to-bore ratio S/B.

The engine was a boosted GDI engine, in line with the current automotive market. To pursue the paper focus, two PROOF-of-CONCEPT engines were designed by CAD at the University of Bologna, based on the trend of current engines: the baseline configuration had unitary S/B ratio for both target powers. The largest bore engine was designed first: the other was derived by scaling the first to preserve the ducts design.

The paper was organized as follows:

1. Two target powers were identified;
2. Based on the today car market, for each target power the bore and the engine speed at maximum power condition were defined. The engines have both unitary S/B ratio and the same BMEP.
3. Analysis aimed to verify if it is possible to increase the two engine strokes, once set the maximum average piston speed at 19.5 m/s, to enhance the thermal efficiency as much as possible, was performed.
4. Once found the best geometric solution for each target power, the variation of the compression/expansion ratio was studied or by the increase of the geometric CR or by the application of over-expanded cycles or both.
5. Finally the water injection strategy in the PWI configuration was applied to the most promising cases, which were found to need a mixture cool down due to the high thermal regime.

It is to say that the over-expanded cycles were applied for both enhancing the thermal efficiency and cooling down the mixture temperature. The focus of the paper was also to determine if these cam timing strategies have the same effectiveness and eventually the same drawbacks on the two engine types.

TOWARD THE RIGHTSIZING ENGINE DESIGN: 0D-ANALYSIS

As stated before, the purpose of the work was to trace the development guidelines useful for the engine design as a function of the target power and therefore of the type of engine (identified by the engine parameter S/B). Two target maximum engine powers were identified:

1. 120 kW at 5500 rpm;
2. 290 kW at 7000 rpm.

At which two bores could correspond, respectively:

1. 75 mm;
2. 84 mm.

In Table 1 the main engine specifications were resumed. It is to say that the maximum average engine speed was set at 19.5 m/s and the BMEP was the same for the two engines. The two basic engines have different CR values: the engine equipped by the smallest bore (75 mm) can adopt a CR greater than the engine having bore of 84 mm because of the reduced knock risk, which is linked to the shorter flame free path.

The first analysis was aimed to identify the best stroke for each engine, pursuing the long stroke engine concept for enhancing the thermal efficiency.

Table 1. Main specifications of the basic engine

Target Power P_{TARGET} [kW]	290.00	120.00
Bore B [mm]	84.00	75.00
Number of Cylinders N_{CYL} [-]	4.00	3.00
Power/cylinders [kW/CYL]	72.50	40.00
Engine speed n [rpm]	7000.00	5500.00
S/B [-]	1.00	1.00
Stroke S [mm]	84.0	75.0
Total swept volume V_c [cm^3]	1862.00	994.00
Unitary swept volume V_{cu} [cm^3]	466.00	331.00
Specific power $P_{SPECIFIC}$ [kW/l]	156.00	121.00
Average piston speed C_m [m/s]	19.50	13.75
BMEP [bar]	26.70	26.40
CR [-]	1:9.50	1:10.00
Conrod Length [mm]	165.60	165.60
Intake valve diameter [mm]	30.24	27.00
Exhaust valve diameter [mm]	28.00	25.00
Intake valve diameter to bore ratio [-]	0.36	0.36
Exhaust valve diameter to bore ratio [-]	0.33	0.33
Squish Height at TDC [mm]	1.10	1.10

Engine stroke increase

The increase of the engine stroke, for given bore, is the first means for increasing the thermal efficiency. The main advantages are:

1. Turbulence increase;
2. Reduction of the ratio Su/V, which reduces the wall losses and increases the reaction rate due to a more suitable surface-to-volume ratio of the flame front.

The main constraint to this stroke increase is the maximum average piston speed, fixed at 19.5 m/s due to mechanical stress issues.

The parameters having a motoristic interest and variable with the stroke increase are (the measurements units and the explanation of the symbols are in Table 1 or in the Appendix):

$$V_{cu} = \frac{V_c}{N_{CYL}} \quad (3)$$

$$C_m = \frac{2 \cdot S \cdot n}{6 \cdot 10^4} \quad (4)$$

$$BMEP = 4 \cdot \frac{P_{TARGET}}{C_m \cdot \frac{\pi}{4} \cdot B^2 \cdot N_{CYL}} \cdot 10 \quad (5)$$

$$P_{SPECIFIC} = \frac{P_{TARGET}}{V_c} \cdot 10^3 \quad (6)$$

There are two main lines of analysis for finding the maximum engine stroke, once imposed the constraint of the maximum average piston speed:

1. Constant bore: this seems to be the most interesting analysis. It could be faced as follows:
    a. At constant engine speed (Analysis #1);
    b. Deriving the maximum engine speed once set the average piston speed to the maximum allowed value (Analysis #2);
2. Constant total swept volume: once set the average piston speed to the maximum allowed value, it is possible to define the combination of stroke, bore and engine speed values (Analysis #3). In this case it is to remark the BMEP increase: some comments on it were reported in the corresponding sub-paragraph.

Analysis #1: Fixed Bore B and Engine Speed n

In this analysis the variation of the average piston speed and the BMEP value was checked. The S/B ratio was varied from 1.0 (baseline solution) up to 1.4. In Figures 1, 2, 3 and 4 the trends of specific swept volume, BMEP, specific power and average piston speed versus S/B ratio increase are reported, respectively. The increase of the specific swept volume (Figure 1), as well known, decreases the BMEP value (Figure 2), reducing the risk of knock onset.

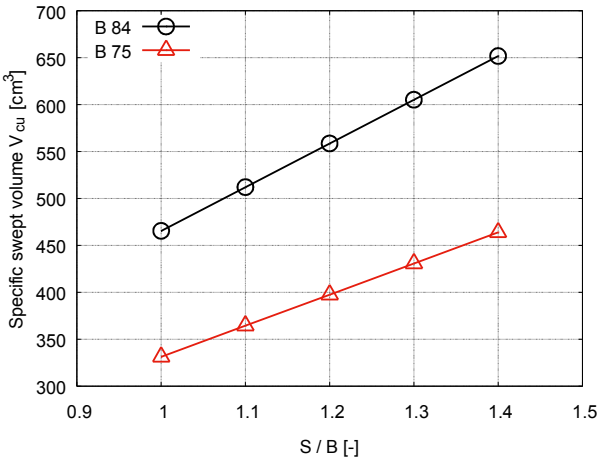

Figure 1. Specific swept volume versus S/B ratio – Fixed bore and engine speed

Moreover, increasing the swept volume and keeping constant the target power, the specific power decreases (Figure 3), which 'lightens' the compressor during transient operation points. As visible in Figure 4, it is not possible to increase the S/B ratio for the engine devoted to power, i.e. equipped by the bore 84 mm, because its average piston speed is already almost equal to the maximum allowed value. Despite the pursuit of thermal efficiency enhancement, an engine characterized by high target power must be equipped by large bore and must run at high engine speed. Thus, there is margin for increasing the S/B ratio, and then the engine stroke, for the engine having the bore 75 mm only.

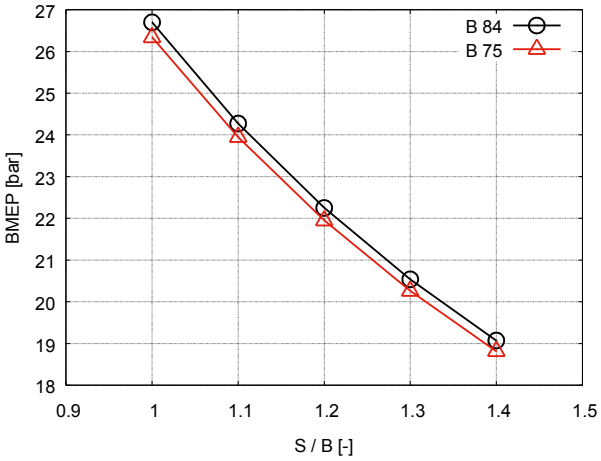

Figure 2. BMEP versus S/B ratio – Fixed bore and engine speed

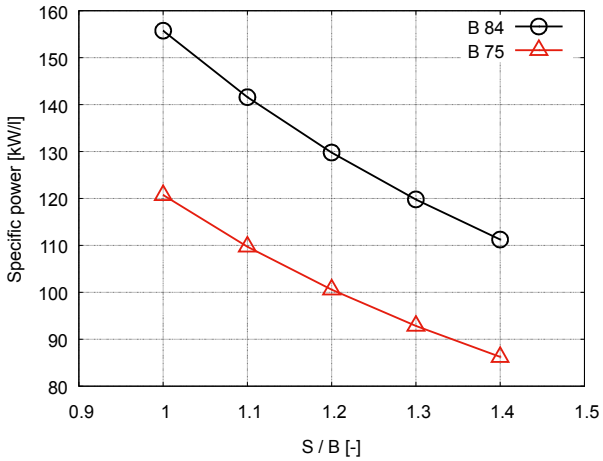

Figure 3. Specific power versus S/B ratio – Fixed bore and engine speed

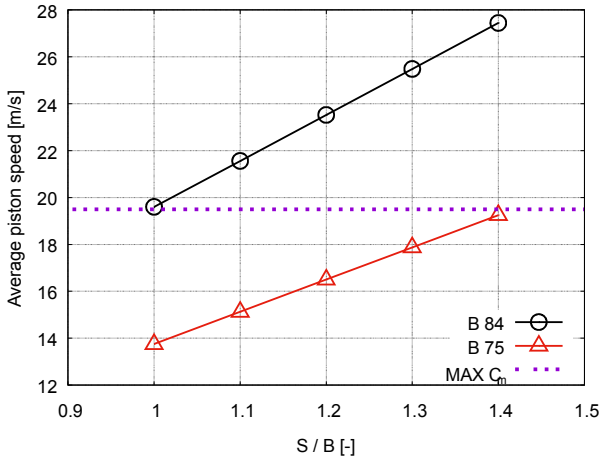

Figure 4. Average piston speed versus S/B ratio – Fixed bore and engine speed

It is to note that the small bore engine (75 mm) can be brought to values of the S/B ratio up to 1.3 or even 1.4, keeping the original bore: at the same engine rotation speed and at the maximum power condition, this leads to a reduction of the engine load, therefore of the BMEP. With the same target power, this design approach has the advantage of reducing the risk of knock: it allows to investigate the possibility of CR increase, as highlighted in Figure 5, where the main advantages / drawbacks of this first analysis were summarized.

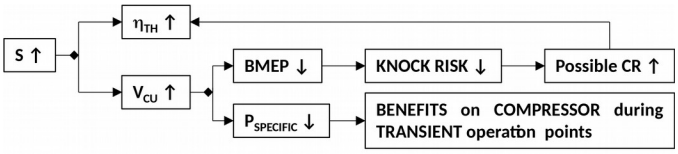

Figure 5. Engine stroke increase effects – Analysis #1

Analysis #2: Fixed Bore B and maximum average piston speed C_{m_MAX}

In this sub-paragraph the variation of the engine speed was checked: keeping constant the bore and the average maximum piston speed, the BMEP is unchanged. The maximum allowed engine speed n_{MAX} (in *rpm*) is derived setting the maximum average piston speed C_{m_MAX} to 19.5 m/s:

$$n_{MAX} = \frac{C_{m_{MAX}}}{2 \cdot S} \cdot 6 \cdot 10^4 \qquad (7)$$

And its trend is visible in Figure 6. For engines equipped by the bore 84 mm, the S/B increase induces a reduction of the engine speed: this solution is not acceptable for a high-power engine design. Besides, it is necessary to consider that:

1. The engine speed decrease leads to a turbulence decrease, partially recoverable by the stroke increase;
2. The engine speed decrease is accompanied by friction reduction for what concerns friction work due to relative motion between moving parts of the engine and engine accessories driving [1].

The engine with bore 75 mm reaches the imposed engine speed of 5500 rpm at S/B ratio equal to 1.4, denoting, as reported in Analysis #1 sub-paragraph, that there is a wide range of design solutions for such an engine: in particular, it is possible to pursue the long stroke concept. The maximum average piston speed, in this case, is reached for S/B=1.0 at engine speed equal to 7800 rpm.

The possibility of keeping fixed the BMEP value by means the reduction of the engine rotation speed is only partially feasible because the average turbulence in the chamber scales with the engine speed and would therefore be penalized, as stated before. However, the turbulence would be partially recovered by the increased stroke of the engine: it is necessary to verify case by case. These last main considerations were resumed in Figure 7.

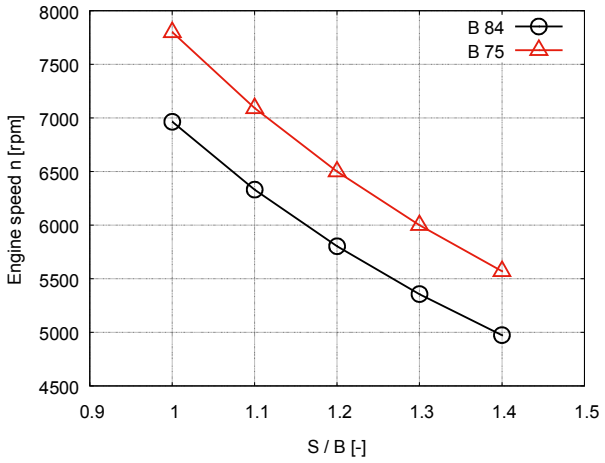

Figure 6. Engine speed versus S/B ratio – Fixed bore and maximum average piston speed

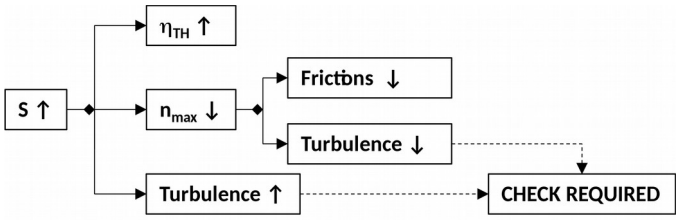

Figure 7. Engine stroke increase effects – Analysis #2

Analysis #3: Fixed total swept volume V_c and maximum average piston speed C_m

The variation of the engine speed and the bore was checked. The bore is derived varying the S/B ratio value from 1.0 to 1.4:

$$B = \left(\frac{V_c}{N_{CYL} \cdot \frac{\pi}{4} \cdot \frac{S}{B}} \right)^{\frac{1}{3}} \quad (8)$$

Once defined the bore B=f(S/B), it is possible to compute the corresponding stroke:

$$S = \left(\frac{S}{B} \right) \cdot B \quad (9)$$

And then the maximum allowed engine speed is estimated by Eq. (7).

In Figures 8, 9 and 10 the trends of engine stroke, speed and bore were reported, respectively. Once fixed the swept volume and the maximum average piston speed, the stroke increase (Figure 8) induces a decrease of both the engine speed (Figure 9) and the engine bore (Figure 10). The engine bore reduction is not acceptable for a high-power engine, especially because the smaller is the bore, the less is the space available for the valves. The proper engine filling is the first focus for getting high-power targets. Beside this, the main drawback is the BMEP increase (Figure 11), which is not affordable because of the consistent increase of the knock risk, together with the decrease of the driveability: this solution must be discarded. In Figure 12 the main results of such an analysis were reported in a scheme.

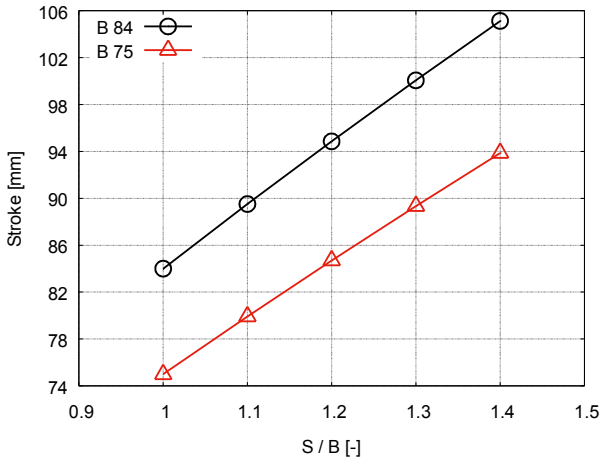

Figure 8. Engine stroke versus S/B ratio – Fixed swept volume and maximum average piston speed

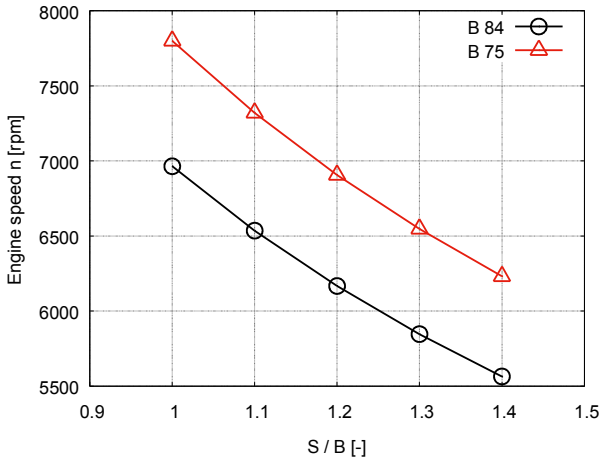

Figure 9. Engine speed versus S/B ratio – Fixed swept volume and maximum average piston speed

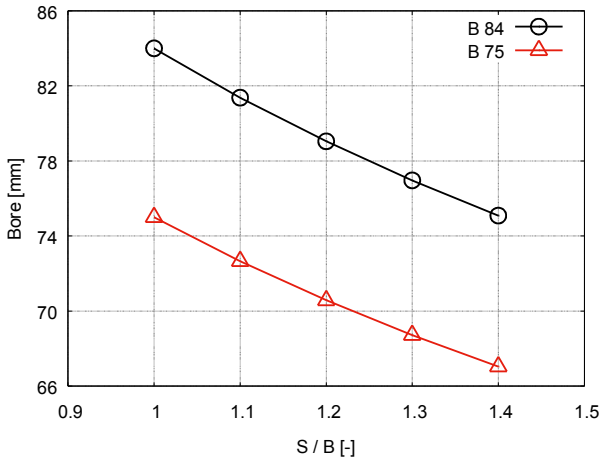

Figure 10. Engine bore versus S/B ratio – Fixed swept volume and maximum average piston speed

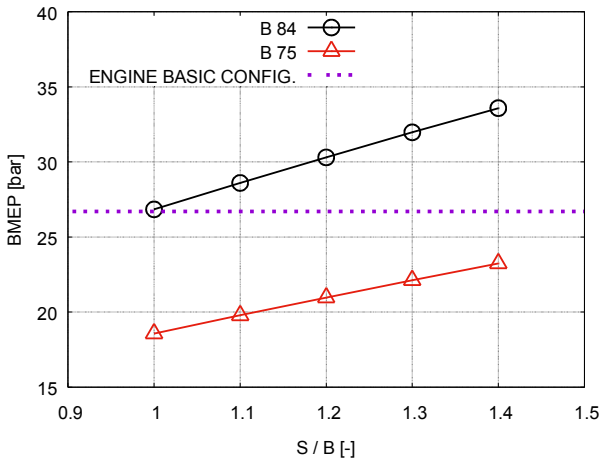

Figure 11. BMEP versus S/B ratio – Fixed swept volume and maximum average piston speed

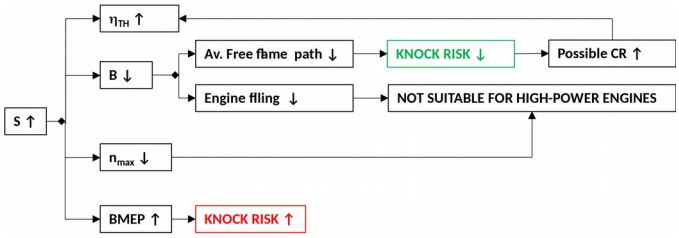

Figure 12. Engine stroke increase effects – Analysis #3

THE ENGINE SPECIFICATIONS

The high-bmep and high-power S.I. GDI turbo-charged engine virtually designed at the University of Bologna is visible in Figure 13a: in Figure 13b is shown the location of the tip end of the GDI injector. It is to note in Figure 13a the position of the port water injector. The injector characteristics were resumed in Table 2 (see [22] for more details). The fuel injector is centrally located (Figure 13b) with a spray targeted to the spark plug for promoting combustion during cat-heating phase.

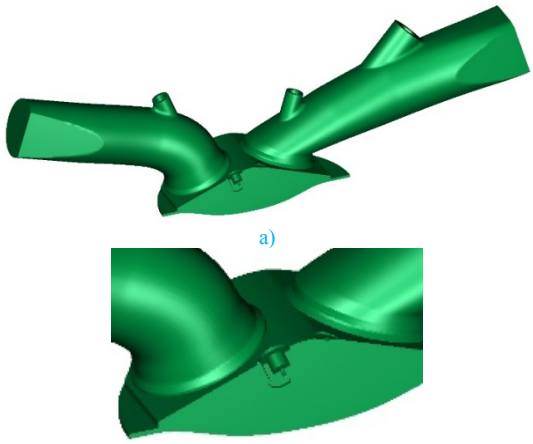

a)

b)

Figure 13. Virtual engine (a) and tip end part of the GDI injector (b)

The operating point in analysis is the full power condition listed in Table 3. The maximum CR for bore 84 mm was 10.5, while it was 12.0 for bore 75 mm, both for geometric constraints.

Table 2. Gasoline injector characteristics

	GASOLINE	PWI [21]
Number of holes [-]	8.0	2.0

Injection pressure [bar]	350.0	10.0
Injection temperature [K]	313.0	313.0
HFR [cm^3/s]	20.0	17.0
Hole geometric diameter [µm]	188.0	347.0

Table 3. Engine operation point at full power – Standard cam timing (STD)

Engine load	100.0%
Mixture index [-]	1.0
Number of valves	4.0
Inlet valve opening [CA deg. ATDC]	362.0
Inlet valve closing [CA deg. ATDC]	598.0
Exhaust valve opening [CA deg. ATDC]	136.0
Exhaust valve closing [CA deg. ATDC]	376.0

DESCRIPTION OF THE SIMULATION ENVIRONMENT

The boundary and the initial conditions for the CFD simulations at the considered operating point were derived by running one-dimensional multi-cylinders simulations using the open source code OpenWAM [24]. The engine cycle three-dimensional CFD simulations, whose setup is shown in Table 4, were performed following a multi-cycle approach: the presented results refer to the last converged engine cycle. Differencing schemes are second order for mass, momentum and energy, while turbulence is resolved with a second order blended scheme. The solution is converged when the residual error for each equation is below the tolerance threshold of 1e-4. Non-reacting flow simulations only were performed and they were stopped at TDC of the converged cycle. Half-geometry domain was considered because of the symmetry conditions. The computational mesh has 506.000 cells at TDC with average cell dimension of 1 mm in the cylinder. A relative humidity of the ambient air of 40% was considered.

The spray modelling technique has been validated and results could be found in [25]. The models adopted for both gasoline and water were the same: the model-specific constants were not tuned differently. In PWI case, only the secondary breakup model was activated: the probability distribution function (PDF) was modified on the basis of a validation process.

All the simulations were run at full load under stoichiometric mixture condition. The reference case, representative of the nowadays fuel-enrichment strategy, is $\lambda = 0.75$. Its average mixture temperature at Top Dead Center (TDC) represents the reference minimum value which must be reached by the "new engine configurations", running at $\lambda = 1.00$, for limiting both knock risk and TiT. All the simulated cases have the same trapped mass for each bore.

Table 4. Main settings for CFD simulations – NON-REACTING FLOW

Start angle	330 CA deg. ATDC
End angle	720 CA deg. ATDC
Turbulence model	K-z-f
Wall heat model	Hybrid wall treatment
Law of the wall	Han-Reitz [20]
Evaporation model	Spalding
Wallfilm evaporation model	Combined

Wallfilm entrainment model	Schadel - Hanratty
Wallfilm splashing model	Kuhnke
Atomization model	Slightly modified version of the model presented in [26]
Breakup model	

CDF SIMULATIONS RESULTS

For CFD analysis the methodological approach illustrated in *Analysis #1 sub-paragraph* was followed. The results were drawn separately for bore 84 mm and bore 75 mm.

Bore 84 mm

As stated before, the stroke increase for the high-power engine is not pursuable: this type of engine was tested in its baseline configuration only. Thus, for increasing the thermal efficiency of such a large bore engine the CR increase was pursued adopting (Table 5):

a. Over-expanded cycles: Miller and Atkinson cycles were tested on the engine. They bring some advantages: i) reduction of the pumping losses; ii) reduction of the effective CR; iii) decrease of the average temperature of the mixture, which allows to increase further the geometric CR. Different cam timing were tested on the basic engine configuration and the best one was applied on the engine with increased CR.
b. Port Water Injection (PWI): this strategy is useful in cooling down the mixture temperature during the compression stroke [16]. It was applied on both the basic engine configuration and the engine with increased geometric CR. The PWI solution was chosen because is the cheapest solution [22]. The water injector spray targeting was carefully chosen to minimize the wall impingement and therefore to promote the water evaporation within the airstream: the constraint of achieving at least the 90% evaporation of the injected water was pursued. The injection pressure was set to 10 bar and the water injected mass was fixed to 25.2 mg, corresponding to s = 0.3 (ratio between the injected water mass and the stoichiometric fuel mass), following the results reported in [22].

Table 5. CFD simulations map – NON-REACTING FLOW – Engine bore 84 mm – P_{TARGET} 290 kW – Stoichiometric condition – 7000 rpm

Geometric CR [-]	Cam timing	Water Injection [-]
9.5	STANDARD (STD)	-
		10 bar – s 0.3
	MILLER (M1)	-
	MILLER (M2)	-
	MILLER (M3)	-
	ATKINSON (ATK1)	-
10.5	STANDARD (STD)	-
		10 bar – s 0.3
	MILLER (M1)	-

“Operation point” strategies aimed to cool down the mixture: water-injection and over-expanded cycles on basic engine configuration

In Table 6 the main injection parameters of both the fuel-only and the water-added cases were reported at stoichiometric conditions. In Table 7 the cam timing of standard and over-expanded cycles was reported for inlet valve only. Exhaust valve cam timing was kept unchanged from the standard cycle (Table 3), as in Figure 14 where the cam timings are depicted: Early IVC (EIVC) cycles are the Miller cycle, while the Atkinson cycle is the LIVC cycle (Late IVC). Thus these over-expanded cycles are the “modern cycles”, adapted to today’s engine needs. All the simulations were run at fixed trapped air mass, thus the boost pressure was increased in the over-expanded cycles simulations with respect to the standard cam timing (STD), as shown in Figure 15: the more is the boost pressure, the more is the load required to the turbo-charger and thus the overall energy requirement. Three Miller cycles and one Atkinson cycle were tested because the Atkinson cycle showed to be less effective in reducing the mixture temperature at TDC, despite it does not penalize the engine fluid-dynamics as much as the Miller cycle, as discussed below. If the focus is to cool down the mixture temperature for allowing the adoption of an increased geometric CR, the Miller cycle is more suitable than the Atkinson cycle. In Figure 16 the temperature difference (ΔT) trends were plotted at stoichiometric condition versus the REFERENCE CASE λ= 0.75 (namely *L 0.75*) at respectively IVC and TDC for: i) standard cam timing without water injection (namely *L 1.0*); ii) standard cam timing with water injection (namely *L 1.0 PWI s 0.3*); iii) over-expanded cycles M1, M2, M3 and ATK as in Table 7. For the STD cam timing it is to note that:

1. As one can expect, moving from fuel-enrichment strategy (λ 0.75) to stoichiometric strategy (λ 1.00) there is an increment of the mixture temperature, respectively of 5 K at IVC (Figure 16a) and 28 K at TDC (Figure 16b);

2. With water addition, the temperature decrease is -23 K at IVC and -12 K at TDC if compared to λ 0.75. Considering the temperature gain at λ 1.00, the temperature decrease is -28 K at IVC and -40 K at TDC.

Moving to over-expanded cycles, it is to note that:

1. As stated before, the Atkinson cycle (ATK) brings a temperature increase at IVC: the IVC temperature is greater than that at stoichiometric condition for standard cam timing. At TDC the average mixture temperature is comparable to that of the fuel-enriched condition. The Miller cycles (M1, M2 and M3) show to always have a lower temperature of the mixture than that of the standard cam timing at λ 0.75, both at IVC and TDC. The most advanced M1 Miller cycle induces the lowest temperature regime inside the cylinder.

2. The M1 Miller cycle doubles the temperature difference gain at TDC with respect to M2 Miller cycle and almost triples that of the M3 cycle.

3. At TDC the effectiveness in the temperature cool down is comparable for M2 case and STD PWI s 0.3 strategy.

Thus, from a thermodynamic point of view, the water injection brings a benefit for the engine, because it is effective in reducing the mixture temperature. The best Miller cycle is the most advanced one, i.e. M1.

Table 6. Fuel and PWI system main injection parameters

Case λ = 1.0	SOI / EOI [CA deg. ATDC]	Injected mass [mg]

Fuel-only	370.0 / 524.0	84.0
Water-added	293.0 / 433.0	25.20 (s=0.3)

Table 7. Over-expanded cycles vs standard cam timing – Inlet valve

Cam timing	Inlet valve opening [CA deg. ATDC]	Inlet valve closing [CA deg. ATDC]	Maximum valve lift [mm]
STANDARD (STD)	362.0	598.0	9.5
MILLER (M1)		520.0	7.5
MILLER (M2)		535.0	
MILLER (M3)		545.0	
ATKINSON (ATK)		650.0	11.25

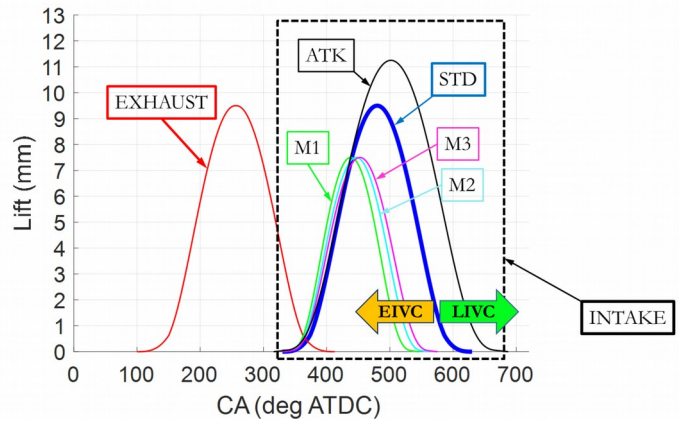

Figure 14. Cam timing

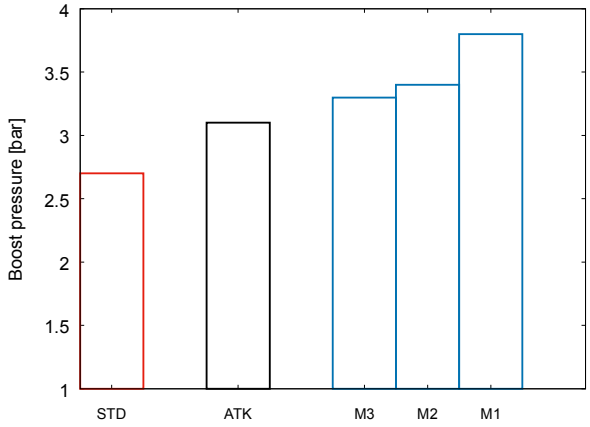

Figure 15. Boost pressure increase

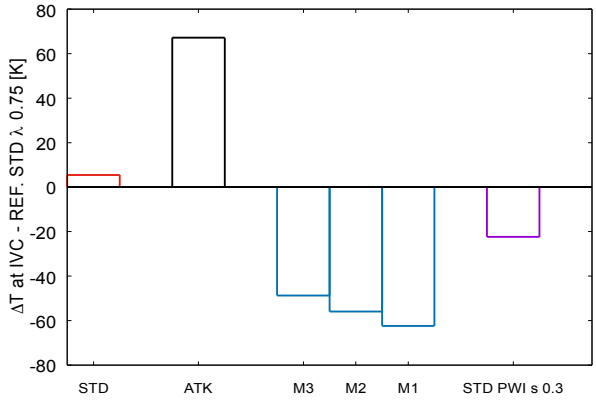

a)

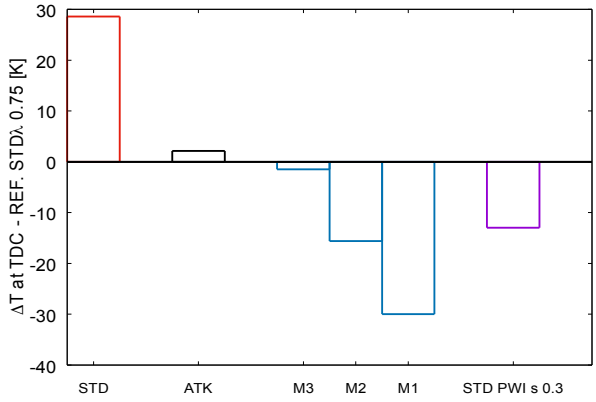

b)

Figure 16. Temperature difference with respect to REFERENCE CASE λ 0.75 at: a) IVC, variable with the adopted cam timing; b) TDC – Stoichiometric condition

Considering the engine fluid-dynamics, in Figure 17 were reported with respect to REFERENCE CASE λ 0.75: i) the percentage variation of the Tumble Ratio TR at IVC, namely *Δ(TR)* in Figure 17a; ii) the percentage variation of the normalized turbulent intensity $\Delta(u'/C_m)$ in Figure 17b, evaluated as the turbulent fluctuating energy *u'* on the average piston velocity C_m, at 710 CA deg. ATDC (i.e. close to optimum ignition time for this type of engine at the full load operation condition).

In Figure 17a the TR at IVC increases as the amount of fuel injected decreases, moving from fuel-enriched to stoichiometric condition, for the same fuel Start Of Injection SOI, because, at least for this engine in this operating condition, the interference between the incoming flow and the momentum of the injected fuel decreases. From λ 0.75 to λ 1.00 the increase is approximately 4.8%. This effect is reduced by adding water: the interference in the duct between the spray and the incoming flow reduces this gain. The TR at IVC remains higher than that at λ 0.75 case but only by about + 1.7%. The turbulence intensity variation in the chamber at 710 CA deg. ATDC follows the same trend of the TR (Figure 17b), except for the Atkinson cycle. The Atkinson cycle penalizes the level of turbulence close to TDC because of the LIVC strategy, which reduces the compression phase of the tumble vortex. Anyway, the Atkinson cycle does not penalize the engine fluid-dynamics as much as all the Miller cycles: the more the Miller cycle is advanced (from M3 to M1), the greater is the penalization on the in-cylinder turbulence close to the ignition time (710 CA deg. ATDC).

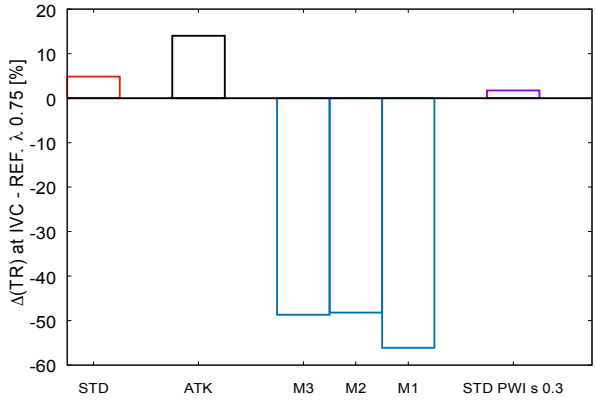

a)

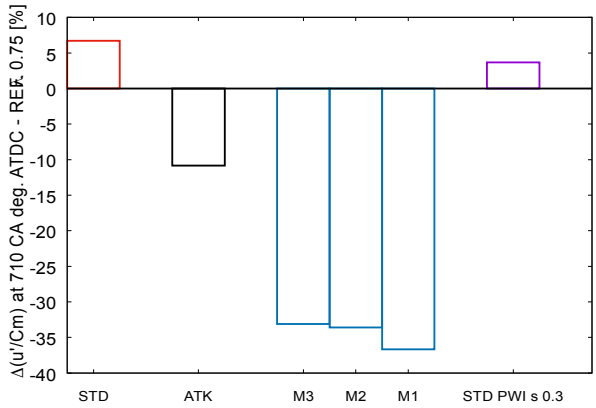

b)

Figure 17. Engine fluid-dynamics behavior with respect to REFERENCE CASE λ 0.75: a) Tumble ratio percentage variation at IVC (which is variable with the cam timing); b) Turbulent intensity percentage variation at 710 CA deg. ATDC

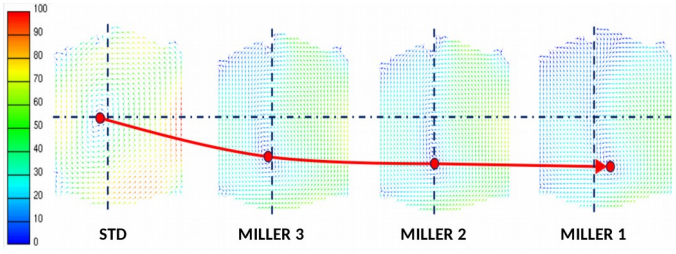

a)

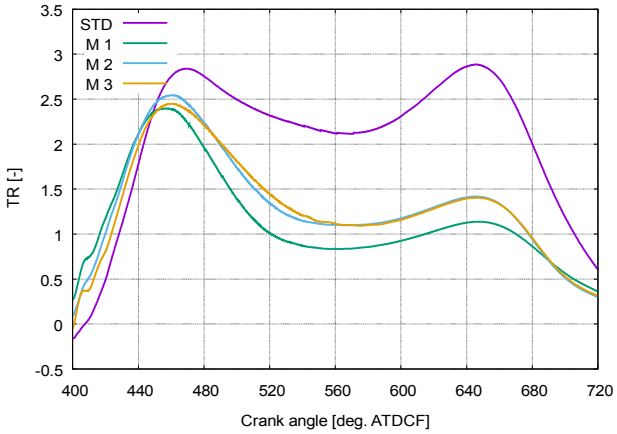

b)

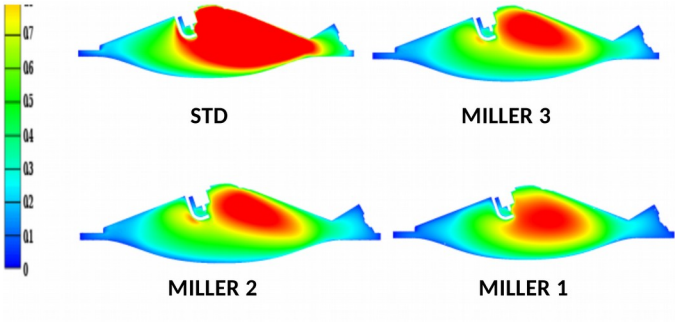

c)

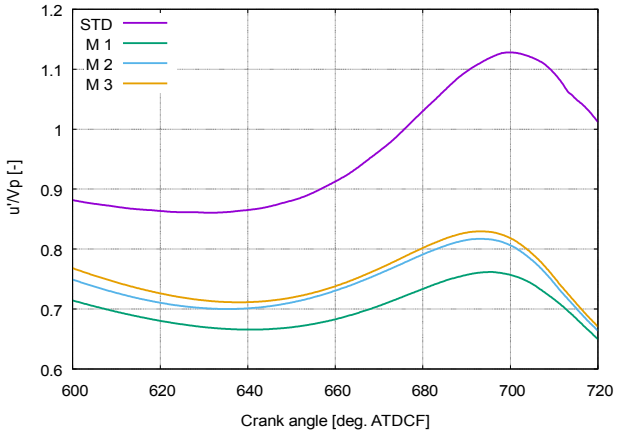

d)

Figure 18. CFD results: a) 3D velocity field at BDC; b) 2D tumble ratio trend; c) 3D turbulent intensity distribution at 710 CA deg. ATDC; d) 2D Turbulent intensity trend – Central tumble plane

For understanding the consistent turbulence penalization related to the adoption of the Miller cycle on such an engine configuration, in Figure 18a the 3D CFD results of the in-cylinder velocity field for standard cam timing (STD λ 1.0) and for the three Miller cycles in analysis were depicted on the tumble plane (which has the axis perpendicular to the cylinder axis) passing through the chamber center at Bottom Dead Center BDC: this picture shows that the main tumble vortex is shifted toward the area below the chamber's center of gravity, the more the IVC time is advanced. The 2D TR trends were reported in Figure 18b, where the TR degradation is evident. Thus advancing the inlet valve closing the main vortex becomes increasingly less coherent: the main consequence is the TR degradation and the turbulence penalization, as visible in the 3D CFD results reported in Figure 18c. Finally in Figure 18d the 2D normalized turbulent intensity trends are visible: the difference between standard and over-expanded cam timing is remarkable. The consistent TR degradation also induces penalization on the air-fuel mixing as in Figure 19, where the air-fuel distribution at 710 CA deg. ATDC was reported. It is well known that the worsening of the mixture index distribution reduces the laminar flame speed: longer 0-10 Mass Fuel Burnt durations and thus larger Coefficient Of Variation (COV) have to be expected, together with enhanced knock risk.

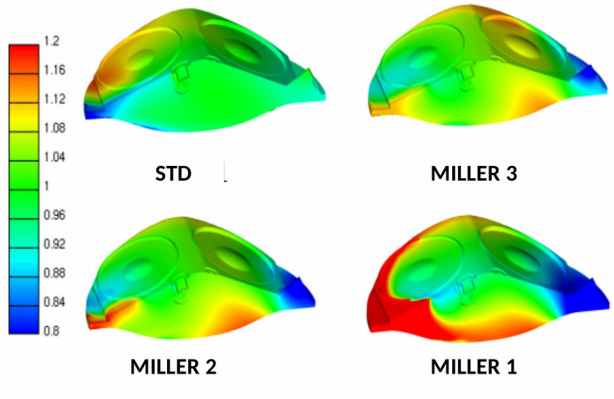

Figure 19. CFD results: air-fuel distribution at 710 CA deg. ATDC

All that being said, the most interesting over-expanded cycle remains the Miller M1 cycle, despite the strongest penalization in the engine fluid-dynamics and in the mixture distribution, as just commented. Besides, it is to mention that one of the main drawbacks of the Atkinson cycle is the possible mixture reflux from the cylinder toward the intake port related to its cam phase. In the next sub-paragraph, the geometric compression ratio increase was tested on STD and M1 cam phases only.

Geometric compression ratio increase

The Miller M1 cycle showed a noticeable cooling effect (Figure 16b). A possible increase in the geometric CR was then analyzed to enhance the thermodynamic efficiency of the engine. It was verified whether the Miller cycle, for an engine with higher CR, has a more or less penalizing effect on the overall engine fluid-dynamics if compared to the basic engine, which works with the Otto cycle and is thus taken as a reference. As in Table 5, the geometric CR was then increased from 9.5 to 10.5 adapting the piston shape, which was flattened.

In Figure 20a the TR trend is visible: the CR increase leads to an even more marked penalization if the engine runs with the Miller M1 cycle. Of consequence the penalization is brought to the turbulence intensity, as in Figure 20b. In particular the TR vortex is penalized in its formation phase because of the flattened shape of the piston, well visible in Figure 21a, where the average velocity field was reported: the vortex center is shifted toward bottom area of the chamber and it is also moved sideways. The result is a strong reduction of the turbulence intensity (Figure 21b) and of the mixing efficiency (Figure 21c). The engine might be more exposed to knock and to larger TiT value due to longer combustion duration.

In this scenario of large-bore engines, designed for high-power densities, the water injection seems to be the most valuable solution because of the strong penalization induced by the Miller cycle in the engine fluid-dynamics and mixture quality distribution. It is also to consider that the boost pressure does not need to be increased with water injection, as in case of over-expanded cycle adoption. Accordingly, it is possible to test the increase of the geometric CR together with the water injection. Authors studied since 2018 the water injection applied to modern GDI engines [14, 15, 21, 22]. In the present work some results only were presented.

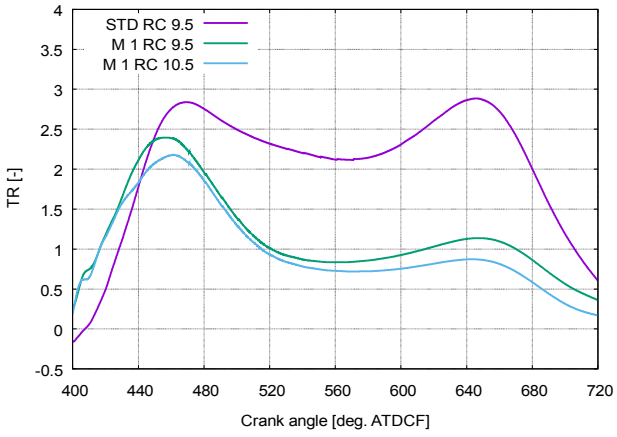

a)

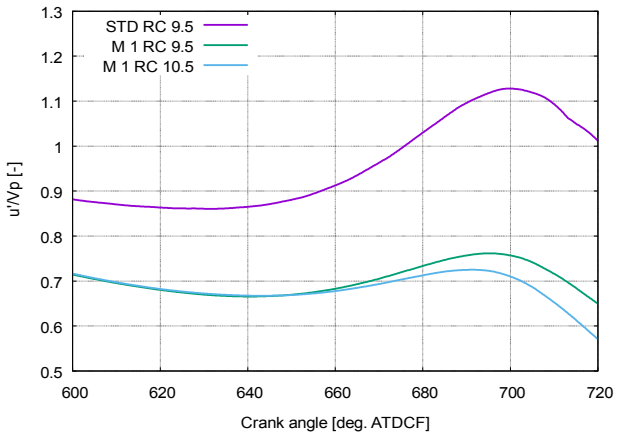

b)

Figure 20. Increased CR: a) Tumble ratio trend; b) Turbulent intensity trend

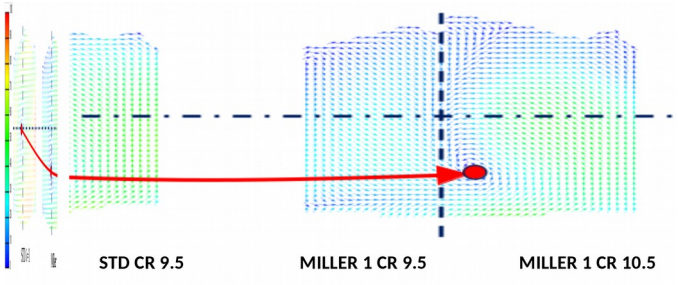

a)

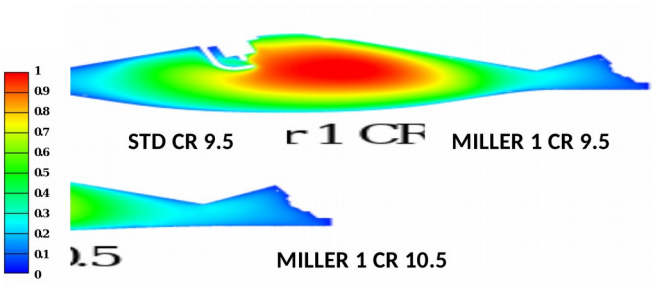

b)

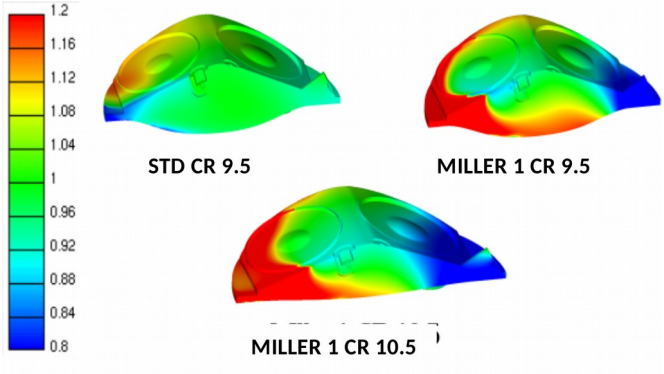

c)

Figure 21. 3D CFD results of CR increase: a) Average velocity field on central tumble plane; b) Turbulent intensity distribution at 710 CA deg. ATDC; c) Mixture index distribution at 710 CA deg. ATDC

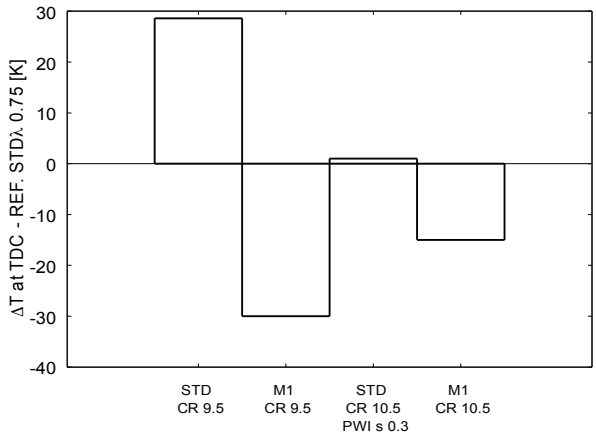

Figure 22. Temperature difference with respect to REFERENCE CASE λ 0.75 STD cam CR 9.5 at TDC – Stoichiometric condition

In Figure 22 the temperature difference trend at TDC with respect to the REFERENCE STD fuel-enriched case (λ 0.75) at CR 9.5 was plotted for the following stoichiometric cases:

1. STD cam and CR 9.5: label *STD CR 9.5* in Figure 22;
2. STD cam, CR 10.5 and water injection (PWI s 0.3): label *STD CR 10.5 PWI s 0.3* in Figure 22;
3. M1 cam and CR 10.5: label *M1 CR 10.5* in Figure 22.

The case with STD cam and CR 10.5, with water addition, was added to this analysis because it is interesting to note that the water injection strategy has a cool down effect comparable to that of the REFERENCE CASE, while the Miller cycle allows to reach an increased temperature cool down at TDC. It is to note that the base case with STD cam and CR 10.5 was not reported because the temperature increase at TDC is an expected consequence of the CR increase. It is more interesting to compare, at CR 10.5, the case with water addition and the case adopting the over-expanded M1 cycle. The case at CR 10.5 and with water addition has a temperature regime at TDC very close to the REFERENCE CASE λ 0.75. The turbulence penalization was reported in Figure 23, where the normalized turbulent intensity percentage variation at 710 CA deg. ATDC with respect to REFERENCE CASE λ 0.75 was plotted for the same cases of Figure 22.

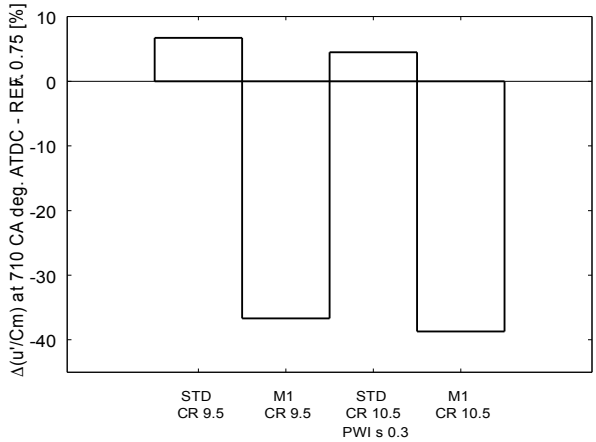

Figure 23. Turbulent intensity percentage variation at 710 CA deg. ATDC with respect to REFERENCE CASE λ 0.75 STD cam CR 9.5 at TDC – Stoichiometric condition

Brief summary of the main findings on the engine equipped by the 84 mm bore

1. GEOMETRIC CONFIGURATION: It is not possible to increase the S/B ratio for this type of engine devoted to power because its average piston speed is already almost equal to the maximum allowed value.
2. ADOPTION OF OVER-EXPANDED CYCLES: The best Miller cycle in terms of mixture cool down is the most advanced one, i.e. M1. The ATK cycle is not as effective as the M1 cycle in the mixture cool down.
3. The ATK cycle slightly penalizes the level of turbulence close to TDC, while the M1 cycle induces always a very strong penalization of the average turbulence level, more than 35% independently by the geometric CR value.
4. GEOMETRIC CR INCREASE: The Miller M1 cycle showed a noticeable cooling effect, thus a possible increase in CR was analyzed. The CR increase led to an even more marked penalization if the engine runs with the Miller M1 cycle. Of consequence the penalization is brought to the turbulence intensity: the result is a strong reduction of the turbulence intensity and of the mixing efficiency too. Moreover, also the CR increase reduces the combustion efficiency because of the non-optimal Su/V ratio of the flame related to the modified shape of the combustion chamber.
5. INJECTION OF WATER: The injection of water, for its part, increased the level of turbulence in this engine (Figure 23) and reduced the temperature at TDC (Figure 22). On the other hand, globally it reduces the laminar flame speed and presents other problems, such as higher cost and difficult market acceptability: Miller cycles are 'transparent to the user', while the water needs at least the filling of the tank. Thus, the optimal solution depends on the specific engine which has to be designed.

Bore 75 mm

The map of the simulation run for the small bore engine B=75 mm is visible in Table 8.

Table 8. CFD simulations map – NON-REACTING FLOW – Engine bore 75 mm – P_{TARGET} 120 kW – Stoichiometric condition – 5500 rpm

Geometric compression ratio [-]	S/B [-]	Cam type	Port Water Injection [-]
10.0	1.0	STD	-
	1.1		-
	1.2		-
	1.3		-
	1.2	M1	-
		M2	-
		ATK1	-
		ATK2	-
		STD	10 bar – s 0.3
		M1	
		ATK2	
12.0		STD	-
			10 bar – s 0.3
		M1	-
			10 bar – s 0.3

All the simulations were run at stoichiometric condition, except the REFERENCE simulation at λ 0.75, as for bore 84 mm, which was run for the best S/B ratio only. For the present engine analysis, the first focus was to increase the S/B ratio finding the best value for the operation condition in analysis: it allows reducing the BMEP and thus the knock, as before commented. Once defined the best S/B ratio, the next simulations were run changing the cam type for testing the effectiveness of the over-expanded cycles on such an engine. The best Miller and Atkinson cycles were run

together with the port water injection for reducing the average mixture temperature, and they were compared to the same engine running with the standard cam law. Finally the geometric compression ratio of the engine running with both the standard cam and the over-expanded Miller cycle M1 was increased for reaching highest thermal efficiency: port water injection was applied for limiting the mixture temperature. The trapped mass was kept constant all over the simulations map, in order to preserve the target power.

Engine stroke increase

The S/B ratio increase needed to design different piston shapes (Figure 24) for preserving the basic CR.

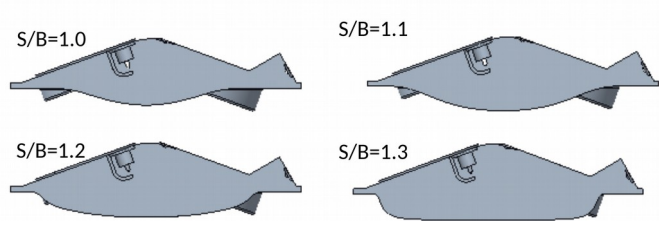

Figure 24. S/B increase – Different piston shapes

It is to note the presence in the chamber of the direct water injector, mounted laterally (on the right side of Figure 24): the engine was designed to run eventually simulations of direct water injection.

Table 9. Engine characteristics

S/B [-]	1.00	1.10	1.20	1.30
Bore [mm]	75.00	75.00	75.00	75.00
Stroke [mm]	75.00	82.50	90.00	97.50
Unitary swept volume V_{cu} [cm^3]	331.34	364.47	397.61	430.74
Combustion chamber volume V_o [cm^3]	36.82	40.50	44.18	47.86
Average piston speed [m/s]	13.75	15.13	16.50	17.88
BMEP [bar]	26.90	23.90	21.90	20.30
Specific power $P_{SPECIFIC}$ [kW/l]	121.00	110.00	101.00	93.00
Boost pressure [bar]	2.40	2.15	2.00	1.85

The tested cases were reported in Table 9: the analysis was then limited to S/B 1.3 to contain the in-cylinder temperature at TDC, as shown below. Increasing the S/B ratio, it is to remark the decrease of the boost pressure for the same trapped mass of air: the less the boost pressure, the less the load required to the turbo-charger. In Figure 25 the temperature difference at TDC with respect to S/B 1.0 case was reported: there is a consistent increase of the temperature at TDC for case S/B 1.3 because of the reduced Su/V of the combustion chamber, as a consequence of the increased S/B ratio. The reduction of the Su/V ratio leads to a reduced wall heat exchange, which increases the average in-cylinder temperature. The temperature increase from S/B 1.2 to S/B 1.3 is particularly consistent: moreover, the decrease of the average in-cylinder pressure (Figure 26) from S/B 1.2 to S/B 1.3 is a consequence of the increased stroke, but it is not enough for helping in knock containment.

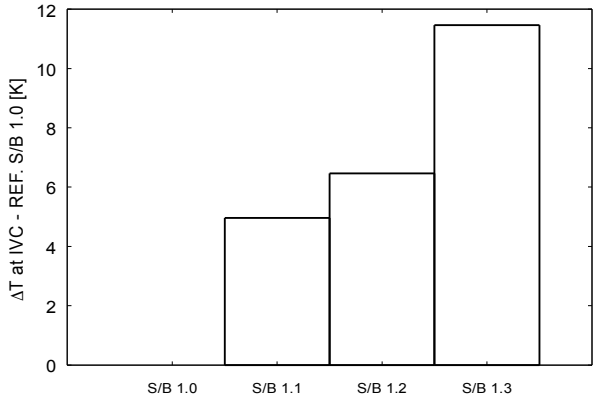

a)

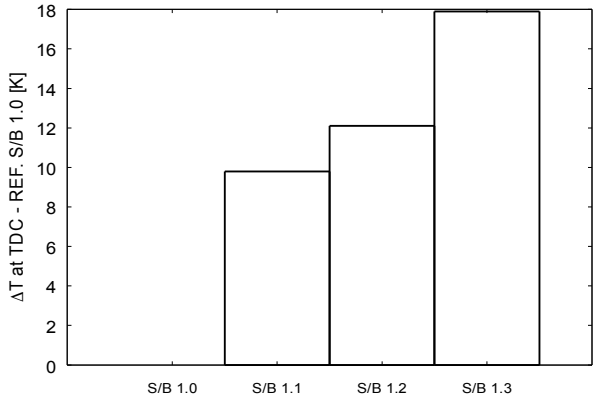

b)

Figure 25. Temperature difference with respect to S/B 1.0 λ 1.0 case at: a) IVC; b) TDC – Stoichiometric condition

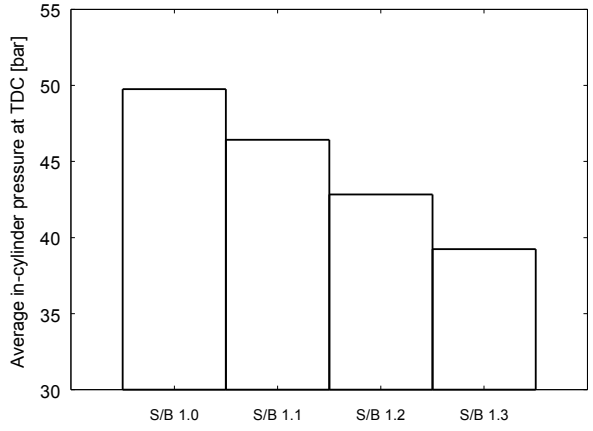

Figure 26. Average in-cylinder pressure at TDC - Stoichiometric condition

In Figure 27 the TR trend is visible: the longer is the engine stroke, the greater is the TR peak. It is also to note that during the spin-up phase (from IVC to the next peak in the TR trend) the difference in the TR trends increases remarkably with the S/B ratio values. In Figure 28 the normalized

turbulent intensity, computed in its percentage variation at 710 CA deg. ATDC with respect to S/B 1.0 case, was plotted increasing the S/B ratio: it is to note that the net increase from S/B 1.1 to S/B 1.2 is greater than the one from S/B 1.2 to S/B 1.3.

For understanding these results of Figures 26 and 27, in Figure 29 the in-cylinder velocity fields a TDC were reported: the velocity fields get stronger increasing the stroke value. In Figure 30 the normalized turbulent intensity distribution at 710 CA deg. ATDC in the central plane was reported: it confirms the results reported in Figure 28.

Finally in Figure 31 the air-fuel distribution at 710 CA deg. ATDC is visible: it is to note the richest value of the mixture index at S/B 1.0 close to the spark plug, while the overall average mixture index value becomes leaner increasing the S/B ratio, up to S/B 1.3.

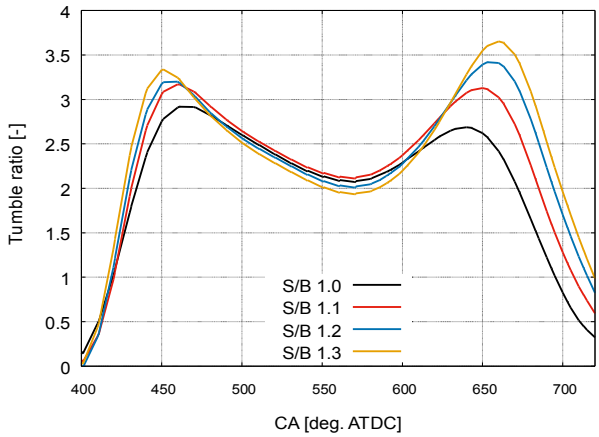

Figure 27. Tumble ratio trend - Stoichiometric condition

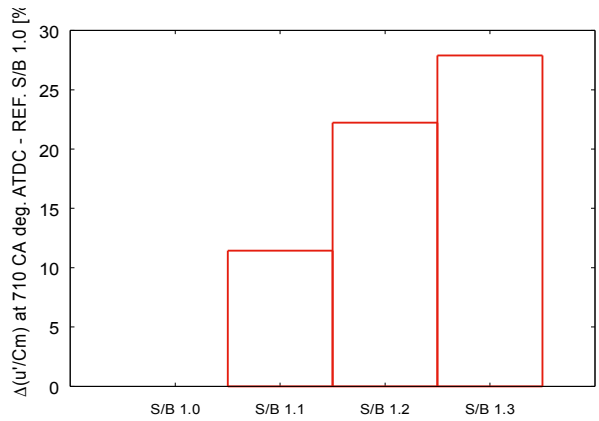

Figure 28. Engine fluid-dynamics behavior with respect to S/B 1.0 λ 1.0 case: Turbulent intensity percentage variation at 710 CA deg. ATDC

Due the above commented results, the best S/B ratio was chosen to be 1.2 for the engine in the analyzed operation point, especially for limiting the average temperature increase at TDC: indeed, the benefits of increasing the stroke / bore ratio from 1.2 to 1.3 (i.e. the turbulent intensity increase) do not compensate for the greater effort in cooling the mixture (due to the strong increase of the mean mixture temperature). The S / B 1.2 solution is more than satisfactory.

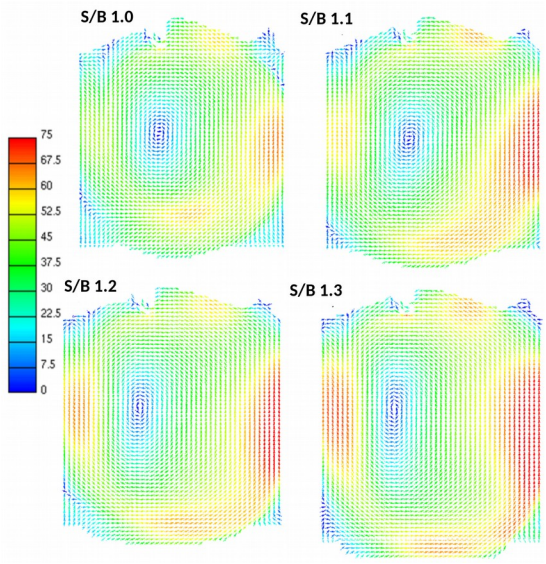

Figure 29. 3D CFD results - Average velocity field – Central tumble plane

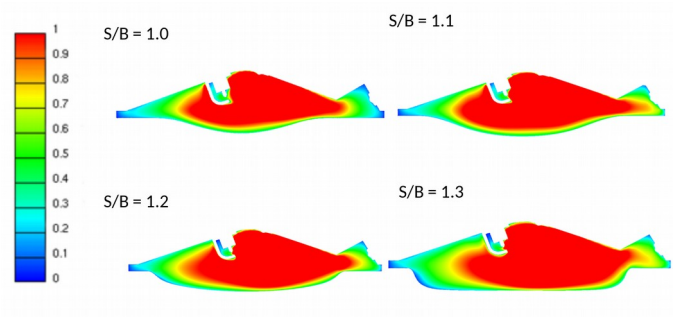

Figure 30. 3D CFD results - Turbulent intensity distribution at 710 CA deg. ATDC – Central tumble plane

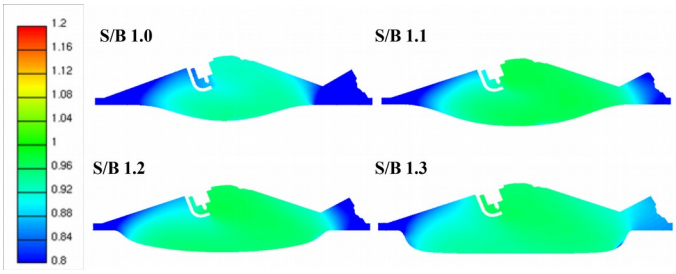

Figure 31. 3D CFD results - Mixture index distribution at 710 CA deg. ATDC

All the remaining simulations were performed at S/B 1.2.

Over-expanded cycles – S/B 1.2

In the present paragraph were reported the results of the simulations performed applying the over-expanded cycles to the best geometric engine configuration, which was chosen to be S/B 1.2 in the previous part of the paper. In fact the configuration having S/B 1.2 is the best trade-off between thermal efficiency enhancement and limited increase of the temperature of the fresh mixture in the chamber at TDC. The REFERENCE case was decided to be the case with STD cam, S/B ratio equal to 1.2, mixture index 0.75. In Table 10 the analyzed cases were resumed: two Miller cycles and two Atkinson cycles were studied, where both the IVC time and the maximum valve lifts were changed.

Table 10. Over-expanded cycles vs standard cam timing – Inlet valve – S/B 1.2

Cam timing	Inlet valve opening [CA deg. ATDC]	Inlet valve closing [CA deg. ATDC]	Maximum valve lift [mm]	Boost pressure [bar]
STANDARD (STD)	362.0	598.0	9.5	2.0
MILLER (M1)		530.0	7.5	2.2
MILLER (M2)		540.0		2.1
ATKINSON (ATK1)		630.0	11.25	2.3
ATKINSON (ATK2)		650.0		2.7

The Figure 32 shows the increase of the boost pressure which becomes necessary moving from the STD to the over-expanded laws of the cam: the most demanding case is the Atkinson ATK 2 cycle. In Figure 33 the temperature difference with respect to the REFERENCE case STD λ 0.75 is plotted: all the over-expanded cycles proved not to be sufficient on their own to lower the TDC temperature at least to the level of the case REFERENCE. Thus, the over-expanded cycles show to need the water addition for the proper cool down of the mixture. If compared to the engine having bore 84 mm, this is due to both the higher value of CR and the increase of the S/B value, which reduces the energy loss at wall, as just commented. The water injection strategy was tested on STD, M1 and ATK2 cycles: the last two are the most performing ones in terms of cool down of the mixture without water addition (Figure 33).

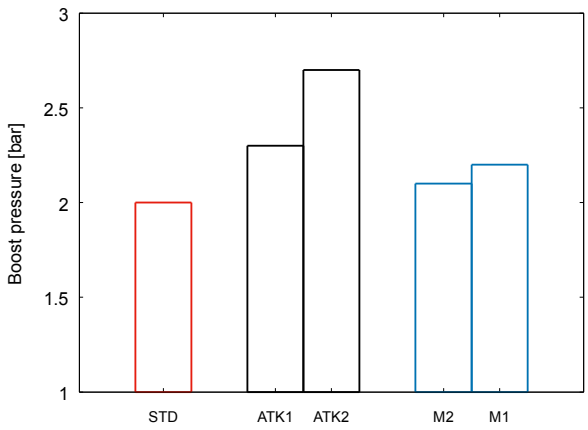

Figure 32. Boost pressure increase due to over-expanded cycles

In Figure 34 the normalized turbulent intensity, computed in its percentage variation at 710 CA deg. ATDC with respect to REFERENCE case, was plotted. It is to note that:

1. With respect to bore 84 mm, the penalty on the engine fluid dynamics is limited;
2. As for bore 84 mm, there is a turbulence decay but less: with B=75 mm the decay is 19%, while with B=84 mm the decay is 38% independently from the CR value.

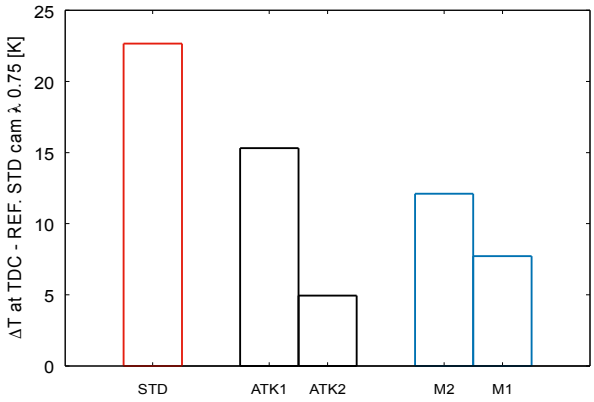

Figure 33. Temperature difference with respect to STD cam λ 0.75 case at TDC – Stoichiometric condition – S/B 1.2

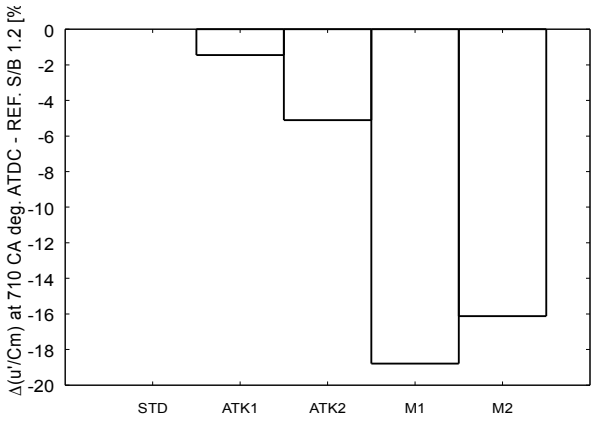

Figure 34. Engine fluid-dynamics behavior with respect to S/B 1.2 STD cam case: turbulent intensity percentage variation at 710 CA deg. ATDC – Stoichiometric condition

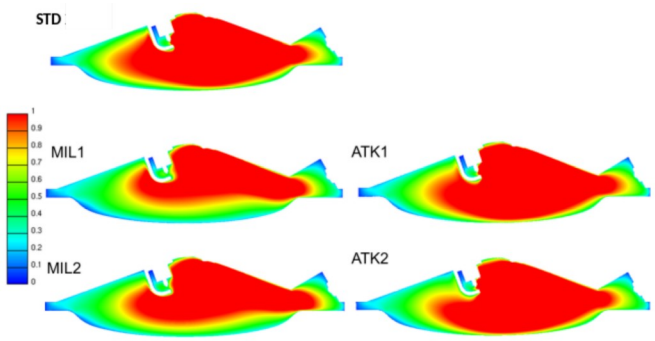

Figure 35. 3D CFD results - Turbulent intensity distribution at 710 CA deg. ATDC – Central tumble plane – S/B 1.2 – Stoichiometric condition

In Figure 35 the normalized turbulent intensity distribution at 710 CA deg. ATDC in the central plane was reported: it confirms the results of Figure 34 above commented.

Water-Injection strategy

As reported in [21], the best PWI solution was found to be the one adopting the injection pressure of 10 bar and a mass of water corresponding to s = 0.3. This case only was tested, as for bore 84 mm, for STD, M1 and ATK2 cam phases (as in Table 8).

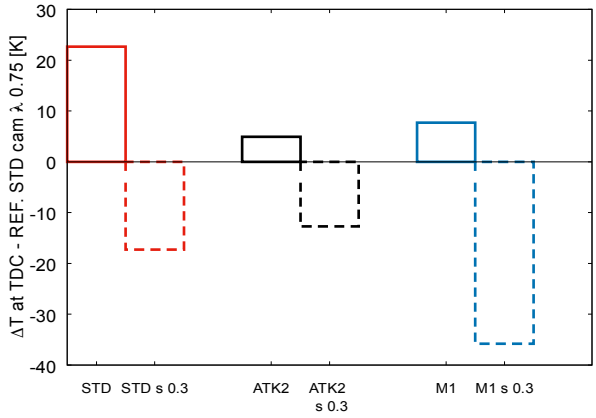

Figure 36. Temperature difference with respect to STD cam λ 0.75 case at TDC – Stoichiometric condition – S/B 1.2

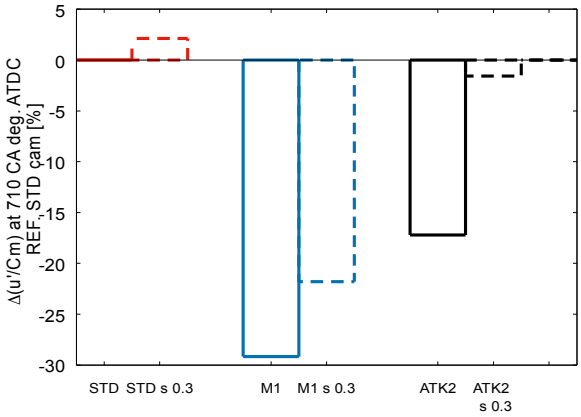

Figure 37. Engine fluid-dynamics behavior with respect to S/B 1.2 STD cam case: turbulent intensity percentage variation at 710 CA deg. ATDC – Stoichiometric condition

In Figure 36 the temperature difference with respect to REFERENCE case is reported: cases with water injection are in dashed line. It is to note the strong temperature decrease obtained with the water injection strategy adoption. As stated before, the over-expanded cycles penalize the normalized turbulent intensity, shown in Figure 37, but the water injection reduces this penalization. Thus the water injection strategy might be a valuable help in reducing the fresh mixture temperature at full load condition.

Geometric compression ratio increase

The CR was increased from 10 of the basic engine to 12. The most interesting cases, analyzed in this sub-paragraph, were:

1. CR 10: STD cam with and without PW injection;
2. CR 10: Miller M1 with and without PW injection;
3. CR 12: STD cam with and without PW injection;
4. CR 12: Miller M1 cam with and without PW injection.

In the figures reported in this paragraph, unless otherwise indicated, the cam is STD. In the x-axis labels the first number indicates the compression ratio, while the water injection is identified by the label *s0.3*. Label *M1* stands for Miller cycle 1. In Figure 38 the temperature difference at TDC with respect to REFERENCE case λ 0.75 CR 10.0 S/B 1.2 STD cam was plotted. It is to note that the water injection strategy is not enough for cooling down the temperature mixture at TDC with CR 12.0: it was necessary to investigate the effect of the Miller cycle M1, despite the already highlighted penalty of the engine fluid dynamics. Case M1 CR 12.0 reduced the average temperature at TDC if compared to the case with STD cam but the temperature was still greater than that of the fuel-enriched case: the M1 cycle was then tested in combination with the port water injection. At higher CR, the only solution capable of reducing the temperature at TDC below the threshold limit (represented by the temperature of the REFERENCE case) was the combined solution of M1 cycle plus PWI water injection strategy.

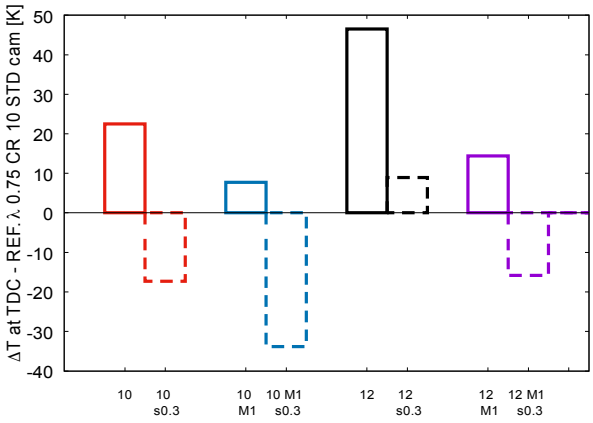

Figure 38. Temperature difference with respect to STD cam λ 0.75 CR 10.0 case at TDC – Stoichiometric condition – S/B 1.2

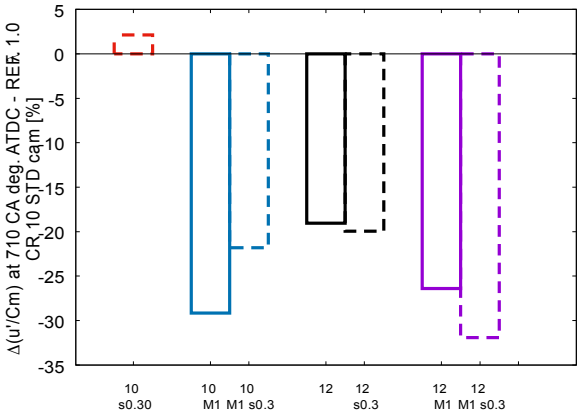

Figure 39. Engine fluid-dynamics behavior with respect to S/B 1.2 STD cam CR 10.0 case: turbulent intensity percentage variation at 710 CA deg. ATDC – Stoichiometric condition

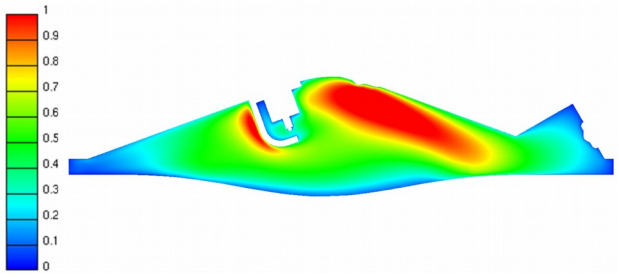

Figure 40. 3D CFD results – Mean turbulent intensity u'/C_m distribution at 710 CA deg. ATDC – Miller 1 and PWI case – CR 12.0

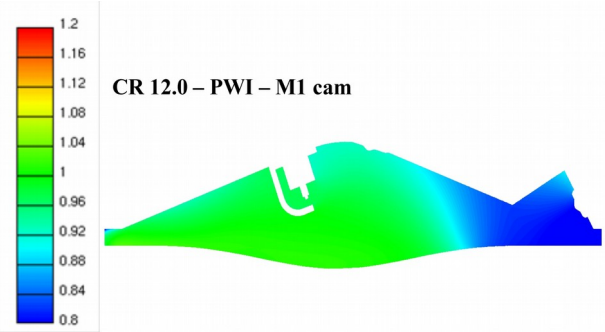

Figure 41. 3D CFD results - Mixture index distribution at 710 CA deg. ATDC – Miller 1 and PWI case – CR 12.0

In Figure 39 for the same cases the normalized turbulent intensity percentage variation at 710 CA deg. ATDC was reported. The geometric CR increase (CR 12.0) induced a decay of the turbulence level close to TDC, not recoverable by the water injection, not even partially.

Unfortunately, the solution at CR 12.0 and adopting the Miller M1 cycle was penalized for the turbulence level at 710 CA deg. ATDC, as well visible in Figure 40 where the turbulent intensity distribution is visible. The distribution of the mixture quality was reported in Figure 41: for Miller M1 PWI case at CR 12 the mixture quality is close to the target stoichiometric value around the spark plug, and it seems to have the optimum value for maximizing the laminar flame speed at the beginning of the combustion process. It might compensate, at least partially, the turbulence decay for the same engine solution. At this point of the research activity, it is mandatory to run simulations under reacting flow conditions: results will be presented in a next paper.

Brief summary of the main findings on the engine equipped by the 75 mm bore

1. GEOMETRIC CONFIGURATION: it is possible to increase the S/B ratio for the engine devoted to energy efficiency (D 75 mm). The increase of the S/B ratio leads to a decrease of the boost pressure for the same trapped mass of air (less load required to the turbo-charger) and to a reduction of the Su/V ratio with a consequent wall heat exchange lowering, which increases the average in-cylinder temperature. The temperature increase from S/B 1.2 to S/B 1.3 is particularly consistent: the decrease of the average in-cylinder pressure due to the increased stroke is not enough for helping in knock containment. Thus the maximum S/B ratio was set to 1.2. Conversely, the S/B ratio increase enhances the level of turbulence close to ignition time;
2. OVER-EXPANDED CYCLES: All the over-expanded cycles proved not to be sufficient on their own to lower the TDC temperature at least to the level of the case REFERENCE. Thus, the over-expanded cycles showed to need the water addition for the proper cool down of the mixture. This is due to both the higher value of CR and the increase of the S/B value, which reduces the energy loss at wall. As for bore 84 mm, they led to a turbulence decay but less: with B=75 mm the decay is 19%, while with B=84 mm the decay is 38% independently from the CR value.
3. WATER INJECTION: there was a strong temperature decrease obtained with the water injection strategy adoption. The over-expanded cycles penalized the normalized turbulent intensity, shown in Figure 37, but the water injection reduced its lowering. Thus the water injection strategy might be a valuable help in reducing the fresh mixture temperature at full load condition.
4. GEOMETRIC CR INCREASE: The geometric CR increase induced a decay of the turbulence level close to TDC, not recoverable by the water injection, not even partially.

CONCLUSIONS

The aim of the work was to trace the development guidelines useful for future engine design as a function of the target power and the engine type, identified by the engine parameter stroke-to-bore ratio S/B. The analyzed engine was a boosted GDI engine, in line with the current automotive market. To pursue the paper focus, two PROOF-of-CONCEPT engines were designed by CAD at the University of Bologna, based on the trend of current engines: the basic configuration had unitary S/B ratio for both target powers. Once defined the two target powers, based on the today car market, for each of them the bore and the engine speed at maximum power condition were defined.

The analysis was carried out following some steps:

5. The first analysis was aimed to verify if it was possible to increase the two engine strokes, imposing the constraint of having the maximum average piston speed set to 19.5 m/s, to enhance the thermal efficiency as much as possible.
6. Once found the best solution for each target power, the variation of the compression/expansion ratio was studied or increasing the geometric CR or applying the over-expanded cycles or both.

7. Finally the water injection strategy in the PWI configuration was applied to the most promising cases, which were found to need a mixture cool down due to the high thermal regime linked to the increase of the CR.

In particular in the paper it was analyzed if the effectiveness of the application of one or more strategies (over-expanded cycles, water injection) was the same for the two engines having two different bores, respectively 84 mm and 75 mm. It is well known that the over-expanded cycles might be detrimental for engine fluid dynamics, despite they could enhance the thermal efficiency of the engine and help in the cool down of the mixture. The comparison between the two engines having bore of 75 mm (S/B 1.2) and 84 mm (S/B 1.0) respectively, gave the following main results:

1. With respect to bore 84 mm, with bore 75 the penalty on the engine fluid dynamics is limited.
2. As shown in Figure 42, where the percentage increase in the boost pressure for both bores 75 and 84 mm compared to the respective REFERENCE case λ 1.0 STD cam is depicted, the Miller cycle required a strong increase of the boost pressure versus the Atkinson cycle at 84 mm. The result was the opposite for the bore 75 mm.
3. In Figure 43, where the percentage variation of the normalized turbulent intensity compared to the respective REFERENCE case λ 1.0 STD cam for both bores 75 mm and 84 mm at CR 9.5 is reported, it is to note that for bore 75 mm there is a turbulence decay but it is limited: for Miller M1 cycle with B=75 mm the decay is 19%, while with B=84 mm the decay is 33%.
4. In Figure 44 the temperature difference compared to the respective REFERENCE case λ 1.0 STD cam with bores 75 mm and 84 mm is illustrated at CR 9.5. It is to highlight how the Miller cycle is much more effective in the mixture cool down that the Atkinson cycle for bore 84 mm, despite its much strong turbulence penalization. In case of bore 75 mm, Atkinson and Miller cycles seem to be almost equivalent. The temperature difference reached with bore 84 mm is stronger than that with bore 75 mm because the last has a S/B ratio of 1.2 instead of 1.0, which limits the energy wall loss, with a consequent increment of the fresh mixture temperature.

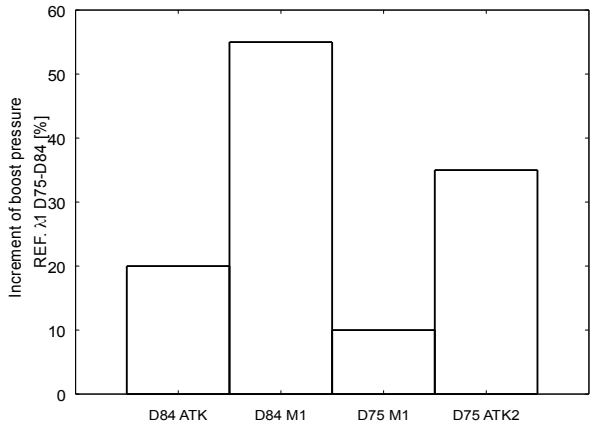

Figure 42. Percentage increase of the boost pressure compared to the respective REFERENCE case λ 1.0 STD cam – Bores 75 mm and 84 mm – CR 9.5

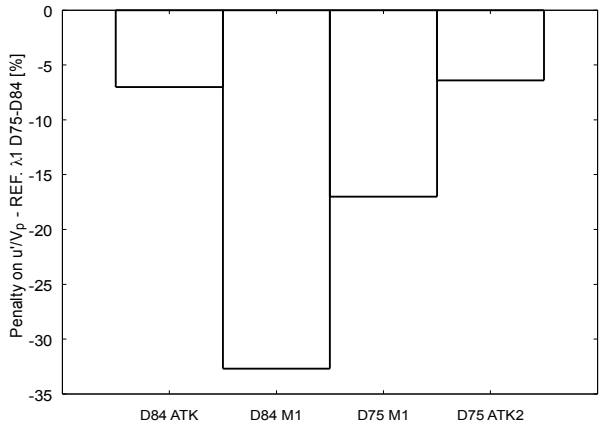

Figure 43. Percentage variation of the normalized turbulent intensity compared to the respective REFERENCE case λ 1.0 STD cam – Bores 75 mm and 84 mm – CR 9.5

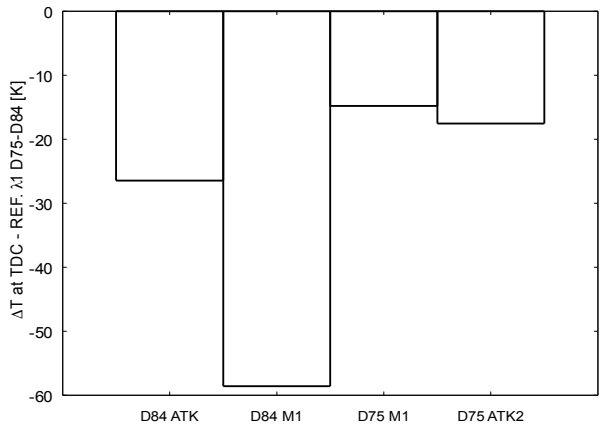

Figure 44. Temperature difference compared to the respective REFERENCE case λ 1.0 STD cam – Bores 75 mm and 84 mm – CR 9.5

Thus, the overall main result was that the 75 mm bore, which might work with a S/B ratio much greater than 1.0, was more suitable for strategies aimed at increasing thermal efficiency of the engine, such as above all the over-expanded cycles. Unfortunately, the engine designed for performance purposes was strongly penalized by the application of the over-expanded cycles, especially in the turbulence level close to ignition time. On the other hand, the long-stroke engine having bore 75 mm suffered a high thermal regime related to the reduced wall losses: the over-expanded cycles, both Miller and Atkinson cycles, are not enough by themselves in lowering the temperature of the fresh mixture and the engine needs the application of the water injection, especially at high CR.

REFERENCES

1. Heywood, “Internal combustion engine fundamentals”, Mc Graw Hill.
2. Shahed, S. and Bauer, K., "Parametric Studies of the Impact of Turbocharging on Gasoline Engine Downsizing," SAE Int. J. Engines 2(1):1347-1358, 2009, https://doi.org/10.4271/2009-01-1472.
3. Nakata, K., Nogawa, S., Takahashi, D., Yoshihara, Y. et al., "Engine Technologies for Achieving 45% Thermal Efficiency of S.I. Engine," SAE Int. J. Engines 9(1):2016, doi:10.4271/2015-01-1896.
4. Smith, P., Heywood, J., and Cheng, W., "Effects of Compression Ratio on Spark-Ignited Engine Efficiency," SAE Technical Paper 2014-01-2599, 2014, doi:10.4271/2014-01-2599.
5. Bunce, M. and Blaxill, H., "Sub-200 g/kWh BSFC on a Light Duty Gasoline Engine," SAE Technical Paper 2016-01-0709, 2016, doi:10.4271/2016-01-0709.
6. Jo, Y., Bromberg, L., and Heywood, J., "Optimal Use of Ethanol in Dual Fuel Applications: Effects of Engine Downsizing, Spark Retard, and Compression Ratio on Fuel Economy," SAE Int. J. Engines 9(2):2016, doi:10.4271/2016-01-0786.
7. Sens, M., Guenther, M., Hunger, M., Mueller, J. et al., "Achieving the Max - Potential from a Variable Compression Ratio and Early Intake Valve Closure Strategy by Combination with a Long Stroke Engine Layout," SAE Technical Paper 2017-24-0155, 2017, doi:10.4271/2017-24-0155.
8. Li, Y., Zhao, H., Stansfield, P., and Freeland, P., "Synergy between Boost and Valve Timings in a Highly Boosted Direct Injection Gasoline Engine Operating with Miller Cycle," SAE Technical Paper 2015-01-1262, 2015, doi:10.4271/2015-01-1262.
9. Osborne, R., Downes, T., O'Brien, S., Pendlebury, K. et al., "A Miller Cycle Engine without Compromise - The Magma Concept," SAE Int. J. Engines 10(3):2017, doi:10.4271/2017-01-0642.
10. Choi, M., Kwak, Y.-H., Song, J., Negandhi, V. et al., “Synergies of Cooled External EGR, Water Injection, Miller Valve Events and Cylinder Deactivation for the Improvement of Fuel Economy on a Turbocharged-GDI Engine; Part 1, Engine Simulation,” SAE Technical Paper 2019-01-0245, 2019, doi:10.4271/2019-01-0245.
11. Choi, M., Kwak, Y.-H., Roth, D.B., Jakiela, D. et al., “Synergies of Cooled External EGR, Water Injection, Miller Valve Events and Cylinder Deactivation for the Improvement of Fuel Economy on a Turbocharged-GDI Engine; Part 2, Engine Testing,” SAE Technical Paper 2019-01-0242, 2019, doi:10.4271/2019-01-0242.
12. Ouyang, X., Teng, H., zeng, X., Luo, X. et al., "A Comparative Study on Influence of EIVC and LIVC on Fuel Economy of A TGDI Engine Part I: Friction Torques of Intake Cams with Different Profiles and Lifts," SAE Technical Paper 2017-01-2245, 2017, doi:10.4271/2017-01-2245.
13. Cao, L., Teng, H., Miao, R., Luo, X. et al., "A Comparative Study on Influence of EIVC and LIVC on Fuel Economy of A TGDI Engine Part III: Experiments on Engine Fuel Consumption, Combustion, and EGR Tolerance," SAE Technical Paper 2017-01-2232, 2017, doi:10.4271/2017-01-2232.
14. Wan, Y. and Du, A., "Reducing Part Load Pumping Loss and Improving Thermal Efficiency through High Compression Ratio Over-Expanded Cycle," SAE Technical Paper 2013-01-1744, 2013, https://doi.org/10.4271/2013-01-1744.

15. S. Falfari, G. M. Bianchi, G. Cazzoli, C. Forte, S. Negro, “Basics on Water Injection Process for Gasoline Engines”, Energy Procedia (2018) pp. 50-57, doi: 10.1016/j.egypro.2018.08.018.
16. Falfari, S., Bianchi, G.M., Cazzoli, G., Ricci, M. et al., “Water Injection Applicability to Gasoline Engines: Thermodynamic Analysis,” SAE Technical Paper 2019-01-0266, 2019, doi:10.4271/2019-01-0266.
17. Lanzafame, R., "Water Injection Effects In A Single-Cylinder CFR Engine," SAE Technical Paper 1999-01-0568, 1999, https://doi.org/10.4271/1999-01-0568.
18. Brusca, S. and Lanzafame, R., "Water Injection in IC - SI Engines to Control Detonation and to Reduce Pollutant Emissions," SAE Technical Paper 2003-01-1912, 2003, https://doi.org/10.4271/2003-01-1912.
19. Bhagat, M., Cung, K., Johnson, J., Lee, S. et al., "Experimental and Numerical Study of Water Spray Injection at Engine-Relevant Conditions," SAE Technical Paper 2013-01-0250, 2013, https://doi.org/10.4271/2013-01-0250.
20. D'Adamo, A., Berni, F., Breda, S., Lugli, M. et al., "A Numerical Investigation on the Potentials of Water Injection as a Fuel Efficiency Enhancer in Highly Downsized GDI Engines," SAE Technical Paper 2015-01-0393, 2015, doi:10.4271/2015-01-0393.
21. Pauer, T., Frohnmaier, M., Walther, J., Schenk, P. et al., “Optimization of Gasoline Engines by Water Injection,” in: 37th International Vienna Motor Symposium, 2016.
22. Falfari, S., Cazzoli, G., Ricci, M., Forte, C., “PWI and DWI Systems in Modern GDI Engines: Optimization and Comparison; Part I: Non-Reacting Flow Analysis”, *accepted for publication to WCX SAE 2021*, SAE paper 2021-01-0461
23. Pulga, L., Falfari, S., Bianchi, G., Ricci, M. et al., "Advanced Combustion Modelling of High BMEP Engines under Water Injection Conditions with Chemical Correlations Generated with Detailed Kinetics and Machine Learning Algorithms*," SAE Int. J. Adv. & Curr. Prac. in Mobility* 3(1):77-94, 2021, *https://doi.org/10.4271/2020-01-2008*.
24. Openwam website. CMT-Motores T ́ermicos. Universidad Polit ́ecnica de Valencia. www.openwam.org.
25. Matteo Ricci, PhD Thesis, University of Bologna, 2020, “Numerical Assessment of the Water Injection Application to GDI Engines”.
26. Brusiani, F., Bianchi, G., and Tiberi, A., “Primary Breakup Model for Turbulent Liquid Jet Based on Ligament Evolution,” SAE Technical Paper 2012-01-0460, 2012, https://doi.org/10.4271/2012-01-0460

Contact Information

For further information/details please contact:

Dr. Stefania Falfari: stefania.falfari@unibo.it

Prof. Gian Marco Bianchi: gianmarco.bianchi@unibo.it

Definitions/Abbreviations

AFR	Air-Fuel Ratio: it is the mass ratio of air to fuel present in the combustion process
AFR_{STECH}	Stoichiometric Air-Fuel Ratio: it is the mass ratio of air to fuel present in the combustion process at stoichiometric condition
ATDC	After Top Dead Center Firing
BMEP	Brake Mean Effective Pressure [bar]
B	Engine bore [m]
BSFC	Brake-specific fuel consumption [g/kWh]
CA	Crank angle
C_m	Average piston speed [m/s]
CR	Geometric Compression ratio [-]